ISSN 0869-5938, Stratigraphy and Geological Correlation, 2020, Vol. 28, No. 1, pp. 1–34. © Pleiades Publishing, Ltd., 2020.
Russian Text © The Author(s), 2020, published in Stratigrafiya, Geologicheskaya Korrelyatsiya, 2020, Vol. 28, No. 1, pp. 3–40.

Mafic Magmatism of Northeastern Fennoscandia (2.06–1.86 Ga): Geochemistry of Volcanic Rocks and Correlation with Dike Complexes

A. A. Arzamastsev[a, b, *], A. V. Stepanova[c], A. V. Samsonov[d], P. K. Skuf'in[e], E. B. Salnikova[a], A. N. Larionov[f], Yu. O. Larionova[d], S. V. Egorova[c], and K. G. Erofeeva[d]

[a] *Institute of Precambrian Geology and Geochronology, Russian Academy of Sciences, St. Petersburg, 199034 Russia*
[b] *Institute of Earth Sciences, St. Petersburg State University, St. Petersburg, 199034 Russia*
[c] *Institute of Geology, Karelian Science Center, Russian Academy of Sciences, Petrozavodsk, 185910 Russia*
[d] *Institute of Geology of Ore Deposits, Petrography, Mineralogy, and Geochemistry, Russian Academy of Sciences, Moscow, 119017 Russia*
[e] *Geological Institute, Kola Science Center, Russian Academy of Sciences, Apatity, 184209 Russia*
[f] *Karpinsky Russian Geological Research Institute, St. Petersburg, 199106 Russia*
**e-mail: arzamas@ipgg.ru*

Received October 31, 2018; revised November 20, 2018; accepted January 25, 2019

Abstract—The comprehensive geochemical and isotopic-geochronological study of Early Proterozoic volcanic rocks in structure of the Polmak–Pechenga–Imandra–Varzuga belt and dikes and sills of the Murmansk and Kola–Norwegian terranes is conducted. Abundant swarms of mafic dikes (2.06–1.86 Ga) are established in the northwestern frame of the belt, including swarms of metadolerites (2060 ± 6 Ma), ferropicrites and gabbronorites (1983 ± 5 Ma), and poikilophitic dolerites (1860 ± 4 Ma). The comparison of volcanic rocks of the Pechenga and Imandra–Varzuga structures shows asynchronous change in volcanism style, with a significant time lapse. The geochemical features of volcanic rocks of the Tominga Formation are typical of those of continental magmatism and can hardly be correlated with those of the Pilguyarvi Formation. According to isotopic-geochronological data, depleted mantle melts in the Pechenga and Imandra–Varzuga zones intruded at 2010–1970 and 1970–1980 Ma, respectively. The analysis of the conditions of formation of volcanic series shows that Neoarchean lithospheric mantle, which produced melts with low Zr/Nb ratios, was a source for primary melts of the Kuetsjarvi Formation of the Pechenga structure and their homologs of the Imandra–Varzuga structure. In contrast, the volcanic rocks of the Kolasjoki Formation, which were weakly contaminated with crustal material, and the related Ilmozero Formation, as well as the metadolerite dikes of the Kirkenes region, were sourced mostly from asthenosphere with separation of melt above the garnet stability depth. The formation of the volcanic rocks of the Pilguyarvi Formation is related, judging from the geochemical data, to two asthenospheric sources different in depth, which produced tholeiitic and ferropicritic melts.

Keywords: Precambrian, dikes, volcanic rocks, Kola Peninsula, Pechenga structure, Imandra–Varzuga structure

DOI: 10.1134/S0869593820010025

INTRODUCTION

Manifestations of Paleoproterozoic mafic magmatism at 2.06–1.86 Ga in the northeastern part of the Fennoscandian Shield are mainly focused in several large structures (Fig. 1), which are combined by many researchers into the Polmak–Pechenga–Imandra–Varzuga (PPIV) belt (Fedotov, 1985; Melezhik and Sturt, 1994; Mintz et al., 1996; Skuf'in et al., 2014; Smolkin, 1997; Smolkin et al., 1995; Zagorodny et al., 1982). Long-term comprehensive studies allowed detailed study of volcano-sedimentary sequences of individual structures of this belt, interpretation of the conditions of formation, and outlining the stages of their formation (Melezhik et al., 2012; Negrutsa, 1984; Predovskii et al., 1987; Skuf'in, 2014, 2018a; Skuf'in and Theart, 2005).

The features of sedimentary, volcanic, and plutonic rocks indicate no evolution of the Pechenga–Imandra–Varzuga structure, which originated at the Archean–Proterozoic boundary (~2.5 Ga) and lasted more than 600 m.y. The transition from continental to oceanic settings with radical change in magmatism was one of the greatest geodynamic events estimated at 2.1 Ga (Hanski, 1992; Hanski and Smolkin, 1989; Hanski et al., 1990, 2014; Sharkov and Smolkin, 1997; Smolkin, 1992). The geochronological (Table 1) and

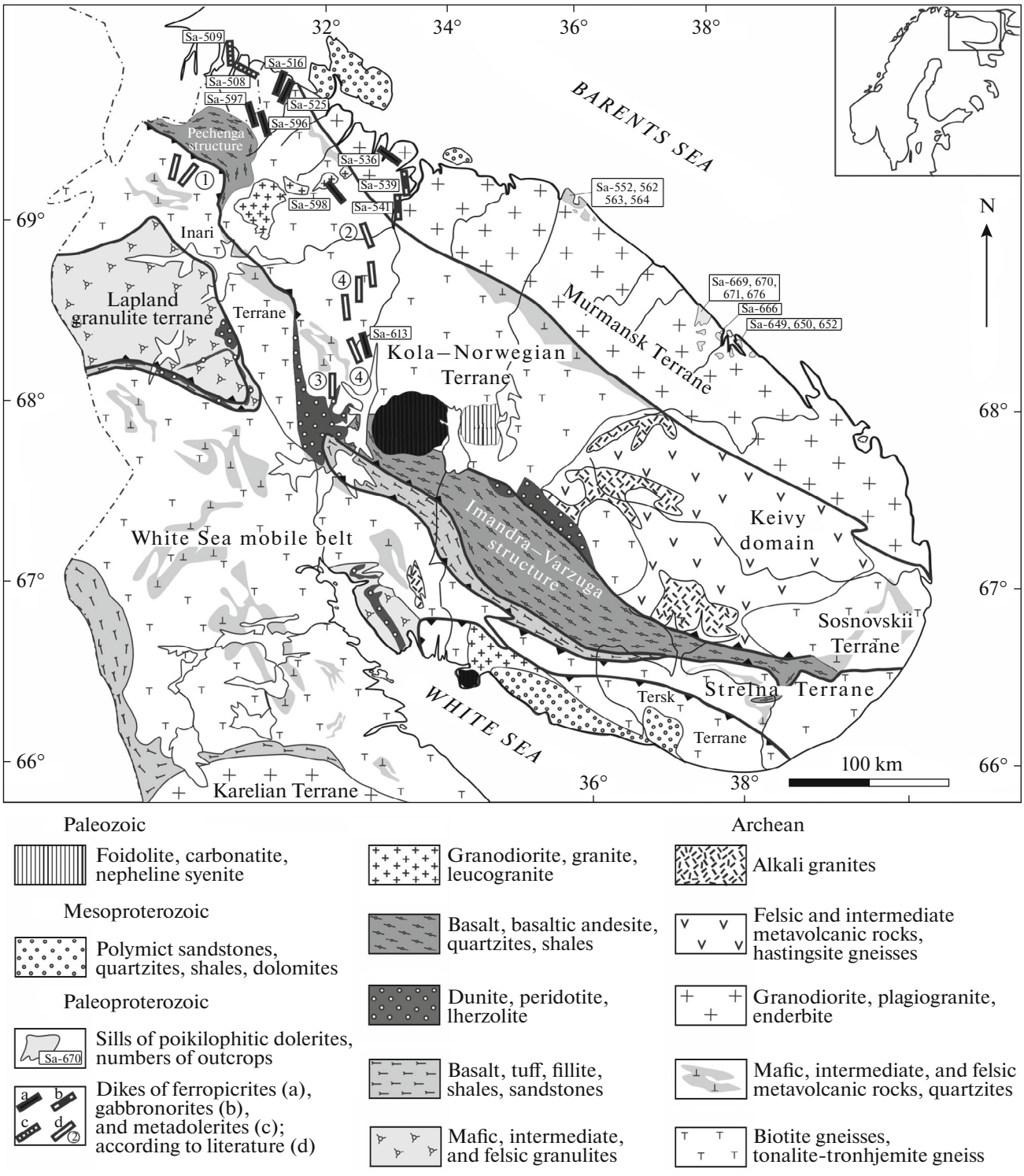

Fig. 1. Schematic geological map of the northeastern part of the Fennoscandian Shield with Early Proterozoic dike magmatism. Numbers in circles show the location of ferropicrite and ferrodolerite dikes according to (1) Yakovlev and Yakovleva, 1989; (2) Borisova, 1989; (3) Nerovich et al., 2014; (4) Fedotov et al., 2012. The geological-tectonic base is after (Daly et al., 2006).

geochemical data (Balashov, 1996; Hanski, 1992; Hanski et al., 1990; Skuf'in, 1993; Skuf'in and Bayanova, 2006; Smolkin, 1992) allow the identification of the main evolutionary stages of the PPIV belt and preliminary correlation of stratigraphic sections and magmatic events within this belt. At the same time, the absence of reliable data on the age of the reference objects, first of all, volcanic rocks in structure of the

Table 1. Geochronological data on volcano-plutonic complexes of the Pechenga–Imandra–Varzuga belt and dike rocks of the Kola–Murmansk block with age of 2.06–1.86 Ga

Pechenga structure			Imandra–Varzuga structure			Swarms of framing dikes		
	age[1]	source		age[1]	source		age[1]	source
South Pechenga	–	–	**Panarechka structure**	–	–	–	–	–
Por'itash complex, dacitic andesite	1904 ± 7[3]	(15)	Saminga Formation, rhyolite	1883 ± 26[3]	(5)	Dal'nie Zelentsy, Poikilophitic dolerite	1860 ± 4[2]	(1)
Kaplya Formation, andesite	1855 ± 40[5]	(13)	Panarechka Formation, trachydacite	1907 ± 18[3]	(5)	–	–	–
Mennel Formation, picrite	1894 ± 40[4]	(10)	Pyalochnozero intrusion, gabbro	1936 ± 9[3]	(17)	–	–	–
Gabbrodolerite	1918 ± 3[3]	(14)	Granite	1940 ± 5[3]	(5)	–	–	–
Granodiorite	1940 ± 17[3]	(4)	–	–	–	North Pechenga, norite	1941 ± 3[2]	(6)
North Pechenga Pilguyarvi Formation	–	–	**Tominga Formation**	–	–	–	–	–
Ferropicrite	1970 ± 5[3]	(8)	Ondomozero intrusion, gabbronorite	1974 ± 6[3]	(17)	Olenegorsk, gabbronorite	1960 ± 3[3]	(7)
Gabbrodiabase	1982 ± 12[3]	(9)	–	–	–	Murmansk, ferrodolerite	1983 ± 5[2]	(1)
Gabbrowherlite	1982 ± 8[3]	(11)	–	–	–	–	–	–
Ferrorhyolite	1988 ± 3[3]	(16)	–	–	–	–	–	–
Ferropicrite	1990 ± 40[4]	(12)	–	–	–	–	–	–
Organic material	2004 ± 9[6]	(18)	–	–	–	–	–	–
Kolasjoki Formation	–	–	**Ilmozero Formation**	–	–	–	–	–
Basalt + clinopyroxene	2018 ± 54[4]	(16)	Volcano-sedimentary sequence, detrital zircon	2052 ± 6[3]	(14)			
Porphyry rhyodacite (sill)	2043 ± 18[3]	(3)				Kirkenes, metadolerite	2060 ± 5[3]	(1)
Kuetsjarvi Formation Volcaniclast, conglomerate	2058 ± 6[3]	(2)	**Umba Formation**	–	–	–	–	–

[1]Age, Ma; [2]baddeleyite, U–Pb method; [3]zircon, U–Pb method; [4]Sm–Nd method; [5]Rb–Sr method; [6]Re–Os method. Sources: (1) original data; (2) Melezhik et al., 2007; (3) Mitrofanov et al., 2001; (4) Melezhik et al., 2012; (5) Skuf'in et al., 2006; (6) Smolkin et al., 2015; (7) Bayanova et al., 1998; (8) Hanski, 1992; (9) Smolkin et al., 2018; (10) Skuf'in et al., 2009; (11) Smolkin, 1999; (12) Smolkin, 1992; (13) Balashov, 1996; (14) Martin et al., 2010; (15) Skuf'in et al., 2014; (16) Hanski et al., 2014; (17) Galimzyanova et al., 2006; (18) Hannah et al., 2006.

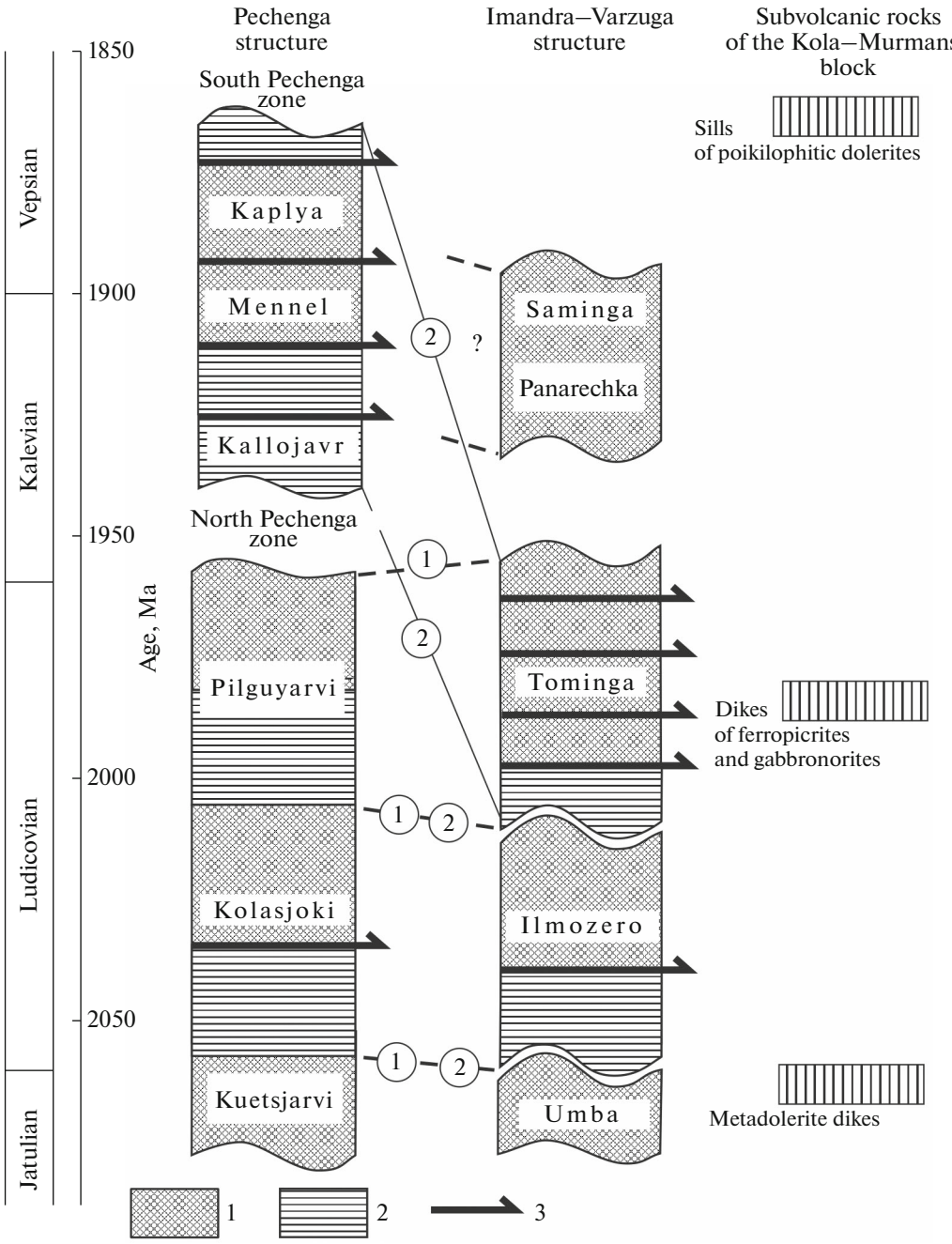

Fig. 2. Correlation of volcano-sedimentary complexes (formations) of the Pechenga and Imandra–Varzuga structures and subvolcanic bodies of the Kola–Murmansk block. Legend: (1) volcanic rocks; (2) sedimentary and volcano-sedimentary rocks; (3) faults. Numbers in circles shows correlation schemes after (Smolkin, 1997) (1) and (Melezhik et al., 2012) (2).

formations, and limited precise geochemical data (Hanski, 1992; Hanski et al., 2014; Melezhik et al., 2012; Mints et al., 1996; Skuf'in and Theart, 2005) hamper the comparison of rock sections (ascribed to the interval of 2.06–1.86 Ga) in Pechenga and Imandra–Varzuga structures, as well as their correlation with sections of the South Pechenga and Panarechka structures (Fig. 2) (Melezhik et al., 2012; Smolkin, 1997; Skuf'in, 2018b). The problem of the scale of magmatism with age of 2.0-6–1.86 Ga on the territory of the northeastern Fennoscandian Shield beyond the volcanic structure is still open.

To solve these problems, we studied the rock-forming (X-ray fluorescence) and trace (ICP-MS) elements of volcanic rocks sampled at various levels of the sections in the age interval of 2.06–1.86 Ga in the Pechenga, Imandra–Varzuga, and Panarechka structures. These data became the basis for comparison and cor-

relation of volcanic parts of the sections in these structures and were used for petrogenetic interpretations.

The petrogeochemical data on volcanic rocks from the upper parts of the sections of the structures of the PPIV belt were compared with data on subvolcanic mafic rocks (dikes and sills) of similar age on the territory of northeastern Fennoscandia. The geochemical correlation of these subvolcanic complexes with volcanic rocks also supports the age of the latter and allows estimation of lateral abundance of mafic magmatism with age of 2.06–1.86 Ga on the territory of northeastern Fennoscandia.

GEOLOGY OF THE REGION

The PPIV belt, which evolved at 2500–1800 Ma and originated on a heterogeneous Archean basement, combines a series of volcanotectonic trough- and graben-like and near-fault depressions, which are filled with volcano-sedimentary rocks, and dividing uplifts and zones of tectonomagmatic activation of the Archean basement (*Seismologicheskaya...*, 1997) (Fig. 1).

The sections of the Pechenga and Imandra–Varzuga structures formed during cyclic-pulsation volcanism, the active periods of which were followed by calm sedimentation. Thus, the basement of each formation in the stratigraphic section is made up of sedimentary rocks, which give way to volcanic rocks up the section. The spatial separation of the Pechenga and Imandra–Varzuga structures and the tectonic setting of rocks significantly hamper the correlation of the Jatulian–Ludicovian part of the section, which is composed of thick volcano-sedimentary sequences in both structures. The correlation schemes (Melezhik et al., 2012; Smolkin, 1997) based on the analysis of the structure of the sedimentary and volcanic parts of the section of the formations are shown in Fig. 2.

Volcanic Rocks of the Pechenga Structure

According to (Melezhik et al., 2012; Predovskii et al., 1987; Skuf'in and Theart, 2005; Skuf'in and Bayanova, 2006; Smolkin, 1992, 1997; Smolkin et al., 1995, 1996), the volcanic rocks with age of 2.06–1.86 Ga intercalated with tuffaceous sedimentary sequences form the main volume of the Pechenga structure, where the Ludicovian rocks of the Pilguyarvi Formation occur on volcanic rocks of the Kolasjoki Formation, which overlap the volcanic rocks of the Kuetsjarvi Formation. The section is crowned by younger volcanic rocks of the Kalevian South Pechenga Group (Figs. 2, 3).

The lower age limit of the Kuetsjarvi rocks has not been identified. The age of 2058 ± 6 Ma was measured for a zircon from a volcaniclastic material occurring in the upper part of the section of the volcanic sequence (Table 1). These data are in agreement with the age of a zircon from a porphyry rhyodacite sill which was drilled by the Kola Superdeep Borehole near the contact with overlying Kolasjoki sedimentary rocks (Mitrofanov et al., 2001), indicating the upper boundary of the formation of 2040–2060 Ma. The lower parts of the Kuetsjarvi Formation are formed by sedimentary rocks with mafic pyroclastics, which occur on Sariolian amygdaloidal basaltic andesites. The composition of sedimentary rocks unambiguously indicates their continental origin (Melezhik et al., 2012; Predovskii et al., 1987; Skuf'in and Theart, 2005). The basement of the volcanic part hosts tuffs and lavas of picrites and ferrobasalts, which gradually give rise to mugearites, subalkali ferrobasaltic andesites, andesites, trachyandesites, ferrous trachydacites, and dacites up the section. Overlying lavas are mostly composed of ferrobasalts with small interlayers of intermediate to felsic tuffs.

The metasedimentary rocks of the Kolasjoki Formation are contrasting in lithology and reflect the transition from terrigenous sedimentation conditions to oceanic settings. If the lower age boundary of rocks of this formation is 2040–2060 Ma, their upper limit may indirectly be determined only from stratigraphic observations and dating results of the Pilguyarvi overlying shales. The volcanic rocks from the upper part of the section of the Kolasjoki Formation include covers of massive and pillow lavas of ferropicrites and basalts, which are intercalated with tuff, tuffaceous shale, and basaltic hyaloclastite layers, as well as with gabbrodolerite beds. The most complete section >1800 m thick was exposed by the Kola Superdeep Borehole (SG-3). The basement of the section contains a horizon of ferropicritic lavas, which are transformed into talc–tremolite–chlorite schists, replaced by basaltic covers up to few tens of meters thick, as well as basaltic sills up to 10–15 m thick.

The lower part of the section of the Pilguyarvi Formation including an ore-bearing gabbrowherlite intrusion hosts rhythmically intercalated layers of greywackes and black carboniferous and sulfide-bearing shales. The maximum Re–Os age of shales of 2004 ± 9 Ma coincides with period of formation of intrusions (Table 1). The upper part of the section is dominated by covers with ferropicritic tuffs, massive and pillow lavas of ferrobasalts, and interlayers of tuffaceous and lava breccias (Predovskii et al., 1974). The lavas contain a thin member of tuffs and ignimbrites of felsic and intermediate to felsic composition, subalkali picrites, and basaltic lavas (Skuf'in, 2014).

The volcanic rocks of the South Pechenga zone are related to the activity of a few autonomous volcanic centers, which yielded the volcanic rocks of bimodal picrite–andesite series. The Mennel Formation combines picrites and alkali and Mg basalts with ultrasilicic ferrorhyolites, which are considered as the analogs of the Pilguyarvi volcanic series (Skuf'in, 2018a; Skuf'in and Theart, 2005). The Kaplya Formation is dominated by subalkali and alkali low-Ti basalts and basaltic andesites. The subvolcanic andesites and dacites of the Por'itash center, which are located along the

contact of the southern and northern parts of the Pechenga structure, could have formed simultaneously with the Kaplya volcanic rocks (Skuf'in and Theart, 2005; Smolkin et al., 1995). The indirect minimum age of volcanic rocks of the South Pechnega zone is 1940–1950 Ma (Skuf'in et al., 2000; Vetrin et al., 2008). The age of volcanic rocks of this zone is a geochronological marker indicating the termination of magmatic events in the Pechenga structure (Skuf'in, 2018a; Skuf'in et al., 2009).

Volcanic Rocks of the Imandra–Varzuga Structure

The Jatulian, Ludicovian, and Kalevian volcano-sedimentary rocks occur in the western and southwestern parts of the Imandra–Varzuga structure, where they form a series of inconsistent horizons with a total thickness of up to 6 km (Fig. 4).

The metasedimentary rocks composing the lower parts of the Umba Formation include red dolomites with picritic pyroclastic, arkose siltstones, and quartz sandstones. They are overlain by subalkali basalts, ferrobasalts, trachyandesites, and picrobasalts, which are replaced by a horizon of picrobasaltic tuffs and lava breccias (Skuf'in, 2014). A regular change in lithofacies of the formation indicates the submergence of the sedimentation area and the increasing role of marine sediments in the eastern part of the Imandra–Varzuga structure (Melezhik et al., 2012). The Kuetsjarvi volcanic rocks are considered as the analogs of the Umba rocks in the Pechenga structure (Fig. 2) (Melezhik et al., 2012; Smolkin, 1997).

The sedimentary rocks of the Ilmozero Formation include carboniferous and sulfide-carboniferous shales, siltstones, silicites, and sulfide-carboniferous tuffaceous sandstones, which indicates a sharp change in sedimentation and, thus, climate and paleogeographical conditions (Melezhik et al., 2012; Predovskii et al., 1974; Skuf'in, 2014). The scarce volcanic rocks of the formation are localized in the central part of the Imandra–Varzuga structure (Fig. 3) and form homogeneous covers of basaltic andesites with features of aerial eruption. The basement of the section contains a horizon of agglomerate subalkali Mg basaltic tuffs.

The relative age of volcanic rocks of the Tominga Formation is based on the geological setting of ferrodolerite dikes similar in chemical composition to volcanic rocks which intrude the Ilmozero rocks (Predovskii et al., 1987). The volcanic rocks mostly include subalkali tholeiitic basalts and Ti and moderately Ti ferrobasalts. The section hosts pillow and massive lavas and ferropicritic sills, as well as thin covers of lavas and tuff dacitic lavas.

The Panarechka caldera (Fig. 4) is a discordant body, which occurs in volcano-sedimentary rocks of the Ilmozero and Tominga formations. The centriclinal concentric bodies of rocks in the periphery surround a core of the structure composed of felsic volcanic rocks with flatter, locally horizontal, dip angles. The volcanic rocks are dominated by basalts, gabbrodolerites, and dolerites (Panarechka Formation) and rocks of monzonite–trachyandesite volcano-plutonic association of a ring fault zone, as well as calc-alkaline dacite–rhyolite association of the Saminga Formation. The age of zircon from plagiomicrocline granite of the internal part of the caldera is 1940 ± 5 Ma and the age of trachydacite from the same structure is 1907 ± 18 Ma (Skuf'in et al., 2006).

Dike Magmatism

The available data on mafic magmatism with age of 2.06–1.86-Ga in the Kola region is mostly limited to data on volcanic rocks and complementary plutonic analogs, which are located within the PPIV belt and in the southeastern continuation of the Pechenga structure, in the Leulik–Kenirim and Tyulpvyd areas (Smolkin et al., 2014, 2018).

At the same time, there are grounds to believe that mafic rocks with age of 2.06–1.86 Ga are more abundant in the northeastern part of the Fennoscandian Shield, which is confirmed by the finds of ferropicrite dikes in the central part of the Kola–Norwegian Terrane and dolerite sills in the Murmansk Terrane, which are supported by geochronological data (Arzamastsev et al., 2009).

Within the Kola part of the Fennoscandian Shield, the subvolcanic intrusions and dikes with age of 2.06–1.86 Ga are mostly localized in the northern part of the PPIV belt. South of this belt, dikes of similar age were found in open pits of the Olenegorsk iron deposit (Nerovich et al., 2014) and in the Allarechka structure,

Fig. 3. Schematic geological structure of the Pechenga structure and its main stratigraphic subdivisions (modified after Smolkin, 1992, 1997; Melezhik et al., 2012; Skuf'in, 2014, 2018a). (1) Granitic rocks of the Litsa–Araguba complex; (2) peridotites and pyroxenites of the Nyasukka dike complex; (3–10) South Pechenga Group: (3) meta-andesites and metadacites of the Por'itash volcanic center; (4) tuffite sandstone of the Kassesjiok Formation; (5) andesites and dacites of the Kaplya Formation; (6) picrobasalts and picrites of the Mennel Formation; (7) tuff and volcanic rocks of the andesite–basalt–picrite composition of the Braginskaya Formation; (8) tuffites of the Kallojavr Formation; (9) granitoids of the Kaskeljavr complex; (10) analogs of rocks of the Pilguyarvi Formation in the South Pechenga Group; (11–15) North Pechenga Group: (11) Pilguyarvi Formation: (a) tholeiitic basalts, ferropicrites, rhyolites; (b) metasedimentary rocks of the Lammas and Zhdanovsky subformations; (12) Kolasjoki Formation: (a) tholeiitic basalts, tuffs, volcaniclastic greywackes; (b) conglomerates, sandstones, jaspers; (13) Kuetsjarvi Formation: (a) basalts, trachydacites, trachyandesites; (b) quartzites and dolomites; (14) Ahmalahti Formation: basaltic andesites and andesites; (15) basal conglomerates and regolite breccias; (16) gabbronorites of Mt. General'skaya; (17) gneisses of the Upper Archean complex; (18) faults; (19) sampling places and numbers of boreholes/outcrops.

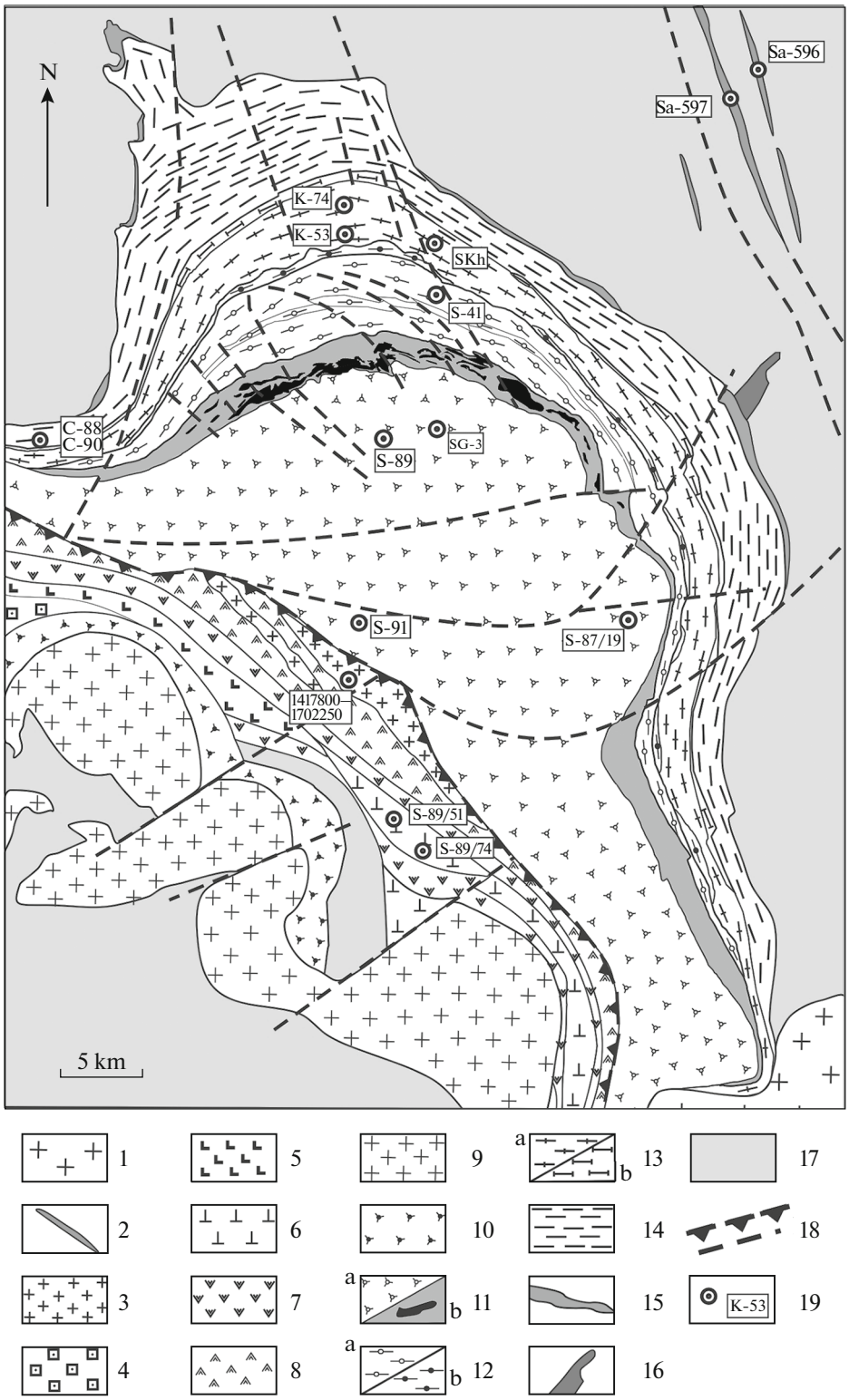

where they form a swarm of longitudinal bodies (Yakovlev and Yakovleva, 1989) (Fig. 1). In terranes adjacent to the belt from the south, including the White Sea mobile belt, folded and boudinaged bodies with age of 2.5–2.3 Ga are dominant amid the Early Proterozoic dikes (Arzamastsev et al., 2009; Balagansky et al., 1986). North of the belt, variously metamorphosed dolerite and ferropicrite dikes are most abundant within the Murmansk Terrane (Fig. 1) and in the adjacent Kola–Norwegian Terrane, where they trace a

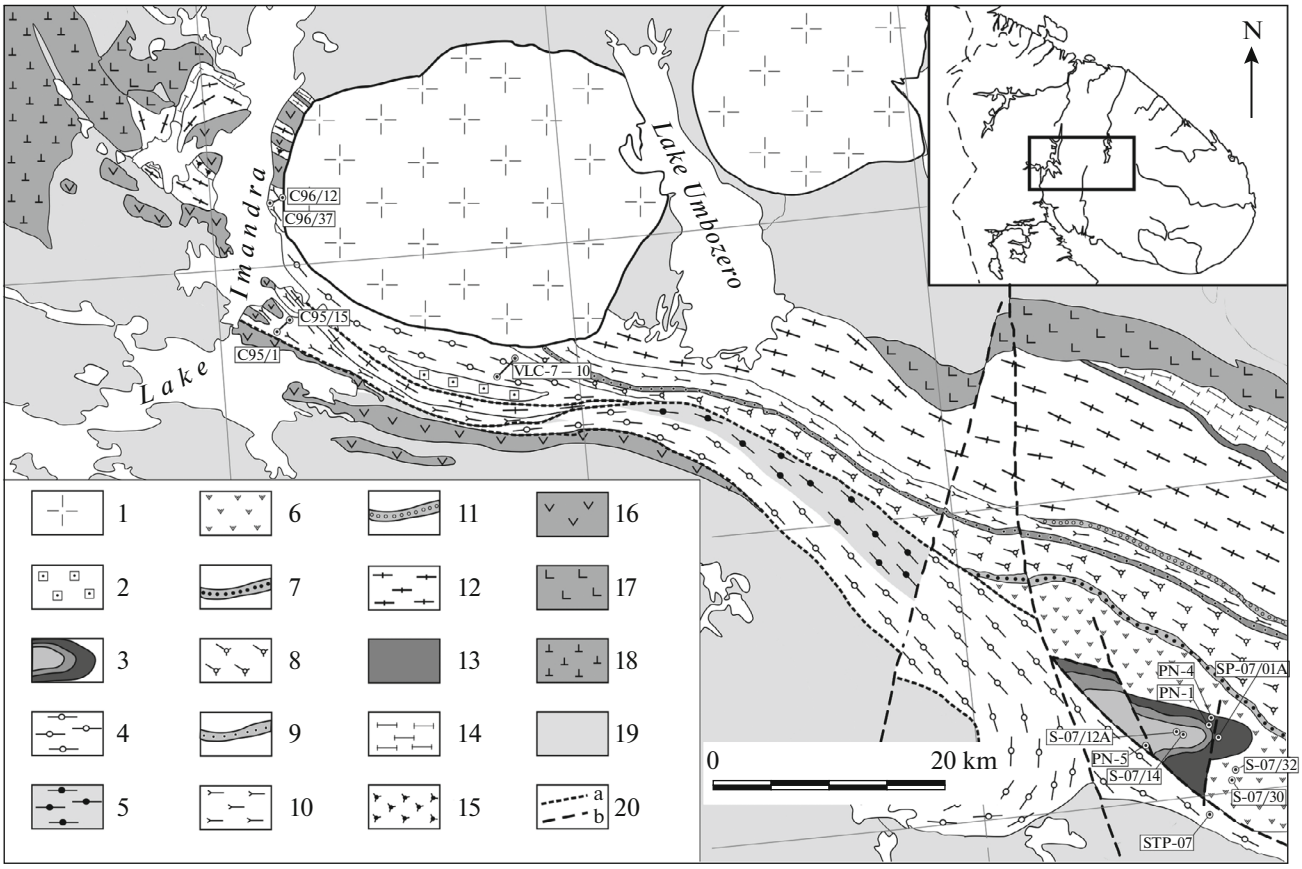

Fig. 4. Schematic geological structure of the western part of the Imandra–Varzuga structure and its main stratigraphic subdivisions (modified after Fedotov, 1985; Skuf'in et al., 2006; Melezhik et al., 2012). (1) Paleozoic: nepheline syenites and foidolites of the Khibiny and Lovozero plutons; (2–18) Proterozoic: (2) alkali syenites of the Soustov pluton; (3) Panarechka Formation; (4, 5) Tominga Formation: unspecified (4) and volcanic (5); (6, 7) Ilmozero Formation: volcanic (6) and sedimentary (7); (8, 9) Umba Formation: volcanic (8) and sedimentary (9); (10, 11) Polisar Formation: volcanic (10) and sedimentary (11); (12, 13) Seidorechka Formation: volcanic (12) and sedimentary (13); (14) Kuksha Formation: quartzites, green schists, greywackes, limestones; (15) granophyres (imandrites); (16) peridotites, pyroxenites, and gabbro of the Imandra intrusive; (17) peridotites, pyroxenites, and gabbro of the Monchegorsk and Fedorovo-Pana intrusions; (18) gabbroanorthosites of the Monchetundra intrusion; (19) gneisses of the Upper Archean complex; (20) unconformable bedding (a), faults (b).

junction zone of the Pechenga and Imandra–Varzuga structures.

The available geochronological data (U–Pb age of baddeleyite and zircon) allow us to distinguish the following groups of subvolcanic bodies of 2.06–1.86 Ga.

Dolerite dikes with age of 2.06 Ga have recently been found in the northwestern part of the Kola–Norwegian Terrane, in the vicinities of the town of Kirkenes and the settlement of Bugøynes (Stepanova et al., 2018). These dikes form two NW-trending swarms. The central and marginal zones of some dikes are composed of gabbrodolerites and fine-grained strongly altered dolerites, respectively. The most crystallized ophitic rocks are composed of clinopyroxene and interstitial plagioclase and quartz and also contain amphibole, biotite, and sericite (Stepanova et al., 2018).

The gabbronorite dikes with age of 1.98 Ga identified by us form several swarms, the largest of which is located east of the Pechenga structure in a wide band within the Kola–Norwegian Terrane (Fig. 1). The steeply dipping dikes of predominantly meridional strike dominate. A few largest dipping dikes, the composition of which corresponds to gabbronorite in the central parts, exhibited differentiation into leucocratic and melanocratic zones. In addition to rock-forming plagioclase and augite, the rocks contain olivine, titanomagnetite, quartz, K-feldspar, biotite, and apatite. Orthopyroxene phenocrysts are present in some dikes. The rocks are strongly amphibolitized.

The ferropicrite and ferrodolerite dikes with age of 1.98 Ga are known in the northern frame of the Pechenga structure and its eastern continuation (Fedotov et al., 2012; Smolkin et al., 2015), in the coastal zone west of the Kola Gulf, and in the lower reaches of the Tuloma River (Borisova, 1989). During our works, the area of occurrence of these dikes was expanded (Fig. 1), and new geochronological, isotopic, and geochemical data on ferropicrite

dikes of the area of the settlement of Liinahamari are given in this paper.

The largest bodies greater than 100 m thick, which are traced for more than 20 km, are part of the Nyasukka dike swarm. They are composed of fully crystalline kaersutite plagioperidotites, olivine plagiopyroxenites, or olivine gabbro. Ferropicrites and their more leucocratic varieties compose smaller bodies (often fully amphibolized). In weakly altered varieties, the microporphyric texture is formed by olivine and augite phenocrysts enclosed in a matrix of augite, plagioclase, magnetite, and ilmenite microlites.

Sills of poikilophitic dolerites with age of 1.86 Ga are abundant within the Murmansk Terrane, in a band from the Boron'ya River to Savikha Bay (Fig. 1) and have similar baddeleyite age in the area of the settlement of Dal'nie Zelentsy (1860 ± 4 Ma) and in the area of Mount Dvorovaya (1863 ± 7 Ma) (Samsonov et al., 2018). The sills form horizontal bodies more than 50 m thick, their top is often eroded, and the lower boundary is often located below the erosion level. In area of Drozdovka, Ivanovka, and Savikha bays, the poikilophitic dolerites form a swarm of vertical dikes of NNE strike along with sills (Fedotov et al., 2012). The sills are weakly differentiated and the upper contact of large bodies is locally composed of coarse-grained quartz gabbrodolerite. The rocks exhibit poikilophitic texture, which is made up of round pyroxene oikocrysts with smaller interstitial plagioclase, biotite, and titanomagnetite crystals.

ANALYTICAL METHODS

The petrogeochemical interpretations and correlations are based on original data on major oxides and trace elements of volcanic rocks of the Pechenga (81 analysis) and Imandra–Varzuga (20 analyses) structures and dike rocks of the Murmansk and Kola–Norwegian terranes (8 analyses). The age was determined for a few reference dike swarms. For comparison, we used a database of more than 1300 published analyses of major oxides of rocks of the PPIV belt. The paper presents the compositions of only representative samples and the complete petrochemical database can be provided upon request.

The contents of major oxides of rocks were determined on an ARL ADVANT'X (Thermo-Scientific) ED XRF spectrometer at the Center for Collective Use of the Karelian Science Center, Russian Academy of Sciences (KarSC RAS). The samples for the analysis were prepared using the following procedure. A 0.3-g sample powder was melted with 3 g of Li tetraborate in a Katanax K1 inductive oven for production of a homogeneous glassy disk. The loss on ignition was measured by gravimetry. The analytical error was 1–5 and up to 12 rel % for oxides with contents of >0.5 and <0.5 wt %, respectively. In some volcanic rocks of the Pechenga structure, the contents of major oxides were determined by atomic absorption at the Geological Institute, Kola Science Center, Russian Academy of Sciences. The analyses were carried out for the same rock sample after its melting with Na tetraborate and soda. The analytical error was no less than ±1.5 and ±3.5% for contents of >10 and >1 wt %, respectively.

The contents of trace (including rare earth) elements were determined using ICP-MS on a Thermo Scientific XSeries 2 mass spectrometer at the Center for Collective Use of the KarSC RAS following the standard method (Svetov et al., 2015). The samples were decomposed by acids in an open system. The analyses were controlled by measurement of standards BHVO-2, AGV-2, and SGD-2A and intralaboratory standard 1412. According to measurement results of standard samples, the relative standard deviation was <5% for most elements, 5.1–6.5% for Sc, V, Cr, Co, Ni, Cu, Zn, and Rb, and 8.1% for Ti.

The Sm–Nd isotopic analysis was conducted in the Laboratory of Isotopic Geochemistry and Geochronology of the Institute of Geology of Ore Deposits, Petrography, Mineralogy, and Geochemistry, Russian Academy of Sciences (IGEM RAS) following the standard method (Larionova et al., 2007). The measurement error of $^{147}Sm/^{144}Nd$ ratio was 0.30% according to the results of measurements of the BCR-1 and BHVO-2 standards.

Baddeleyite and zircon for U–Pb isotopic studies were extracted on a Wilfley concentrating table at the IGEM RAS following the method described in (Söderlund and Johansson, 2002).

The U–Pb age of baddeleyite was determined using ID-TIMS at the Institute of Precambrian Geology and Geochronology, Russian Academy of Sciences. For isotopic analysis, we used the most transparent homogeneous baddeleyite crystals, which were accurately cleaned from surface contaminations in alcohol, acetone, 1 M HNO_3, and 1 M HCl. After each step, the crystals were washed with distilled water. Baddeleyite was decomposed following a modified method of Krogh (1973) in Teflon capsules placed into a Parr reactor system, and the $^{235}U–^{202}Pb$ tracer was added directly before decomposition. Isotope composition was obtained on a TRITON TI mass spectrometer using an ion counter. The error of U and Pb determination was 0.5%. The bulk contamination was less than 1–5 pg Pb and 1 pg U. The experimental data were processed in the PbDAT (Ludwig, 1991) and ISOPLOT/Ex (Ludwig, 2010) programs. The ages were calculated using commonly accepted values of U decay constants (Steiger and Jäger, 1976). Common lead was corrected according to the model values (Stacey and Kramers, 1975). All errors are given at the 2σ level.

The U–Pb Isotope composition of zircon was obtained at the Center for Isotopic Research of the Karpinsky Russian Geological Research Institute (VSEGEI) on a SHRIMP-II ion microprobe following the standard methods (Larionov et al., 2004; Wil-

liams, 1998) using standard zircons 1500 and Temora. The ages were calculated using decay constants from (Steiger and Jäger, 1976) and corrected for nonradiogenic lead according to (Stacey and Kramers, 1975) on the basis of the measured $^{204}Pb/^{206}Pb$ ratio. The results were processed in the SQUID v1.12 (Ludwig, 2005) and ISOPLOT/Ex (Ludwig, 2010) software.

GEOCHEMISTRY OF VOLCANIC ROCKS

On the basis of the chemical composition of rocks of the PPIV belt (Fedotov, 1985; Skuf'in, 2014, 2018a; Smolkin, 1992, 1997; Predovskii et al., 1974), magmatic evolution of the belt is characterized by several active cycles, which resulted in the change of igneous rocks from undifferentiated basalts to felsic calc-alkaline and alkaline derivates. At the same time, the available single geochemical characteristics of rocks indicate a regular change of geodynamic settings, which resulted in specific geochemical features of volcanic rocks formed at each stage of the evolution of the structure. Here, on the basis of new analytical data, we characterize the typical volcanic rocks of the northern and southern parts of the Pechenga structure, as well as the Ilmozero, Tominga, and Panarechka formations of the Imandra–Varzuga structures, which are supplemented by data on dike magmatism.

Volcanic Rocks of the Pechenga Structure

The Kuetsjarvi volcanic rocks are mostly salic with evident alkaline trend (Fig. 5). The alkali sum ($Na_2 + K_2O$) of the most differentiated rocks reaches 9.5 wt %. Subalkaline affinity caused their specific evolution leading to the formation of Fe trachybasalts (mugearites) and Fe trachyandesites at the early stages and Fe trachytes, Fe trachydacites, and Fe dacites at the final stages. The volcanic rocks of the upper part of the section include the ferrobasalt–trachyte series. Its most primitive members are dominated by ferrobasalts, which are high-Ti and high-Fe quartz- and hypersthene-normative rocks, the $Fe_2O_{3\,total}$ and TiO_2 contents of which can reach 20 and 3.2 wt %, respectively (Fig. 5). The rocks of the formation have higher LILE and HSFE contents, which are close to those of E-MORBs. The patterns of trace elements normalized to primitive mantle (Fig. 6a) exhibit negative U, Sr, and Zr minima. The $Nb/Nb^* = Nb_N/[(Th_N)(La_N)]^{1/2}$ ratio, which characterizes the degree of contamination of melts by a crustal component, varies from 0.5 to 1.5. The REE pattern shows significant REE fractionation ($(La/Sm)_N$ = 2.1–4.9, $(Gd/Yb)_N$ = 2.2–2.9) and the absence of Eu anomaly (Eu/Eu^* = 0.91–1.09). The high $(Gd/Yb)_N$ ratios of this rock group indicate their fractionation as a result of melting of a garnet-bearing source. The chemical composition of representative samples is given in Table 2.

The Kolasjoki volcanics comprise tholeiitic basalts and significantly differ from Kuetsjarvi subalkaline rocks in terms of petrogeochemistry. They belong to moderately Ti (0.9–2.0 wt % TiO_2) and ferrous tholeiites with two-pyroxene-normative mineral composition. On MgO–oxide diagrams, the data points of basalts form a trend indicating fractional crystallization of high-Mg basaltic melt with early crystallization of olivine and clinopyroxene and restite plagioclase. The Kolasjoki basalts are characterized by relatively low Ni, Co, and Cr contents (<70 μg/g), the absence of Nb minimum, and negative anomalies of Sr ($Sr/Sr^* \sim 0.45$) and Zr ($Zr/Zr^* \sim 0.75$) (Fig. 6b, Table 3). The weak REE fractionation ($(La/Sm)_N$ = 1.3–1.7, $(Gd/Yb)_N$ = 1.2–1.6) and minor Eu anomaly (Eu/Eu^* = 0.8–1.1) distinguish them from the Kuetsjarvi basalts. A sill of porphyry rhyodacites amid the most differentiated rocks occurring at the contact zone of the Kolasjoki Formation with the underlying Kuetsjarvi Formation is an age marker (Table 2, Sample RIOD) (Mitrofanov et al., 2001). The sill rocks are normal alkaline and peraluminous and are enriched in Fe and Mg. The rhyodacites belong to hypersthene-normative types. In spite of different compositions, nearly coeval metadolerites and rhyodacites show similar negative anomalies of Nb ($Nb/Nb^* \sim 0.15$), Sr ($Sr/Sr^* \sim 0.15$), and Eu ($Eu/Eu^* \sim 0.45$) (Fig. 6d).

The Pilguyarvi volcanic rocks include the basalt–tholeiitic and ferropicrite series, the latter of which is related to the ore-bearing gabbro-wehrlite intrusions (Hanski, 1992; Melezhik et al., 2012; Smolkin, 1992). The highly variable major oxide contents and the presence of hybrid varieties obscure the petrochemical characteristics of rocks of both series (Fig. 5); however, the trace element pattern allows their discrimination (Table 4). For example, in Fig. 6, the tholeiitic basalts are comparable with OIBs in most trace element contents and differ in weakly fractionated REE patterns.

The high contents of TiO_2 (>2 wt %) and Fe_2O_{3total} (>14 wt %) are major differences of rocks of ferropicrite series with dominant picrites and picrobasalts (Fig. 5). All differentiates have significantly higher LILE, HSFE, and REE contents in comparison with those in OIBs and E-MORBs (Fig. 6c), negative Sr anomaly ($Sr/Sr^* \sim 0.16$), and negative Ba and Ti anomalies in most evolved ferrorhyolites. The REE patterns of these rocks are strongly fractionated in both light ($(La/Sm)_N \sim 3.2$) and heavy ($(Gd/Yb)_N \sim 3.0$) domains and have small negative Eu anomalies ($Eu/Eu^* \sim 0.8$; up to 0.6 in ferrorhyolites).

The volcanic rocks of the southern part of the Pechenga structure significantly differ in composition in different volcanic centers. The Mennel Formation is composed of volcanic rocks of the picrite–picrobasalt–basalt–andesite series, the most primitive members of which are close in composition to E-MORBs (Fig. 6e, Table 5). Against the background of widely variable major oxide contents, the most Mg-rich variet-

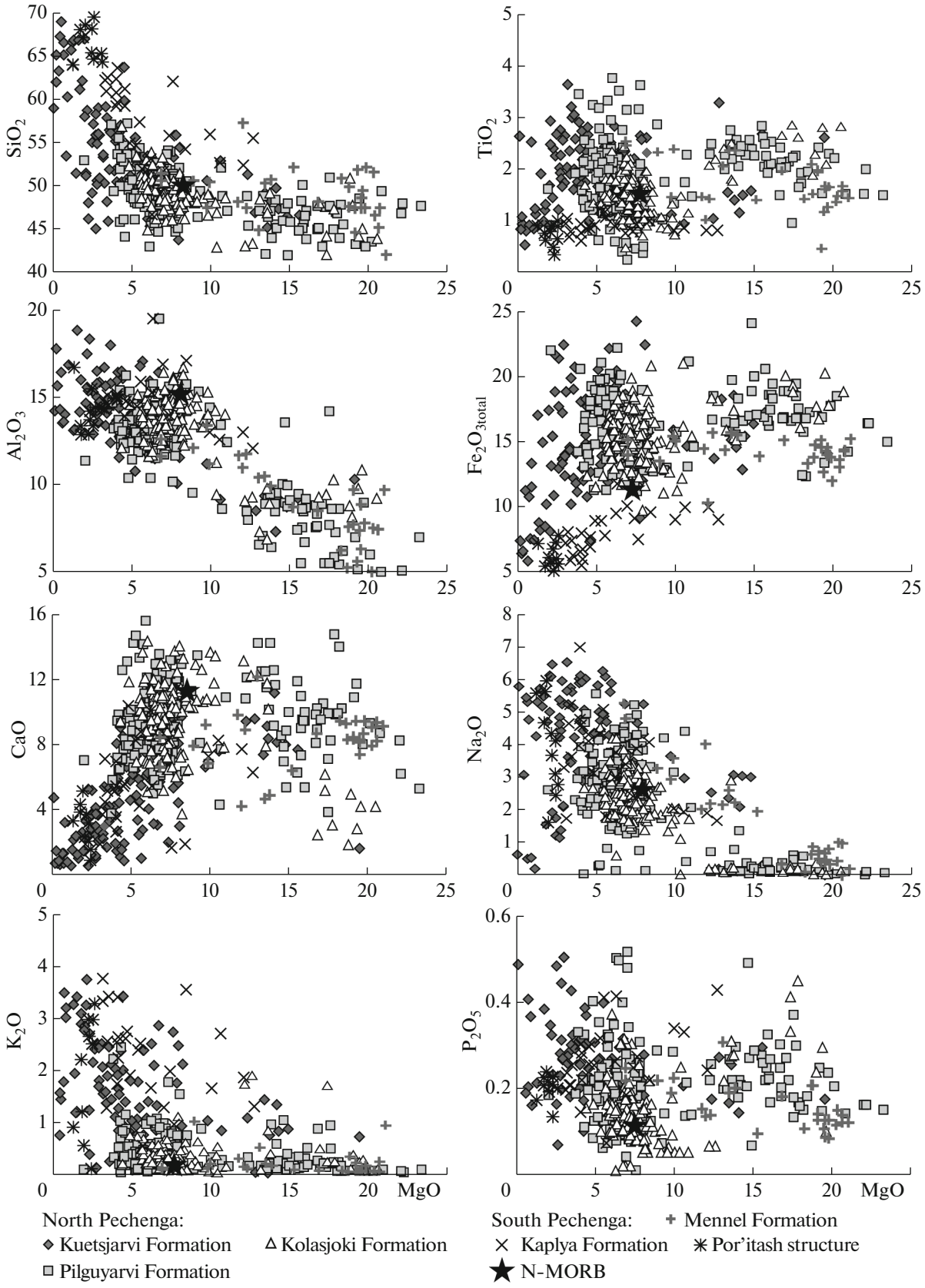

Fig. 5. MgO–oxide plot (wt %) for the Early Proterozoic volcanic rocks of the Pechenga structure on the basis of original and published data (Predovskii et al., 1974; Skuf'in and Theart, 2005; Smolkin, 1992). The N-MORB values are after (Hart et al., 1999).

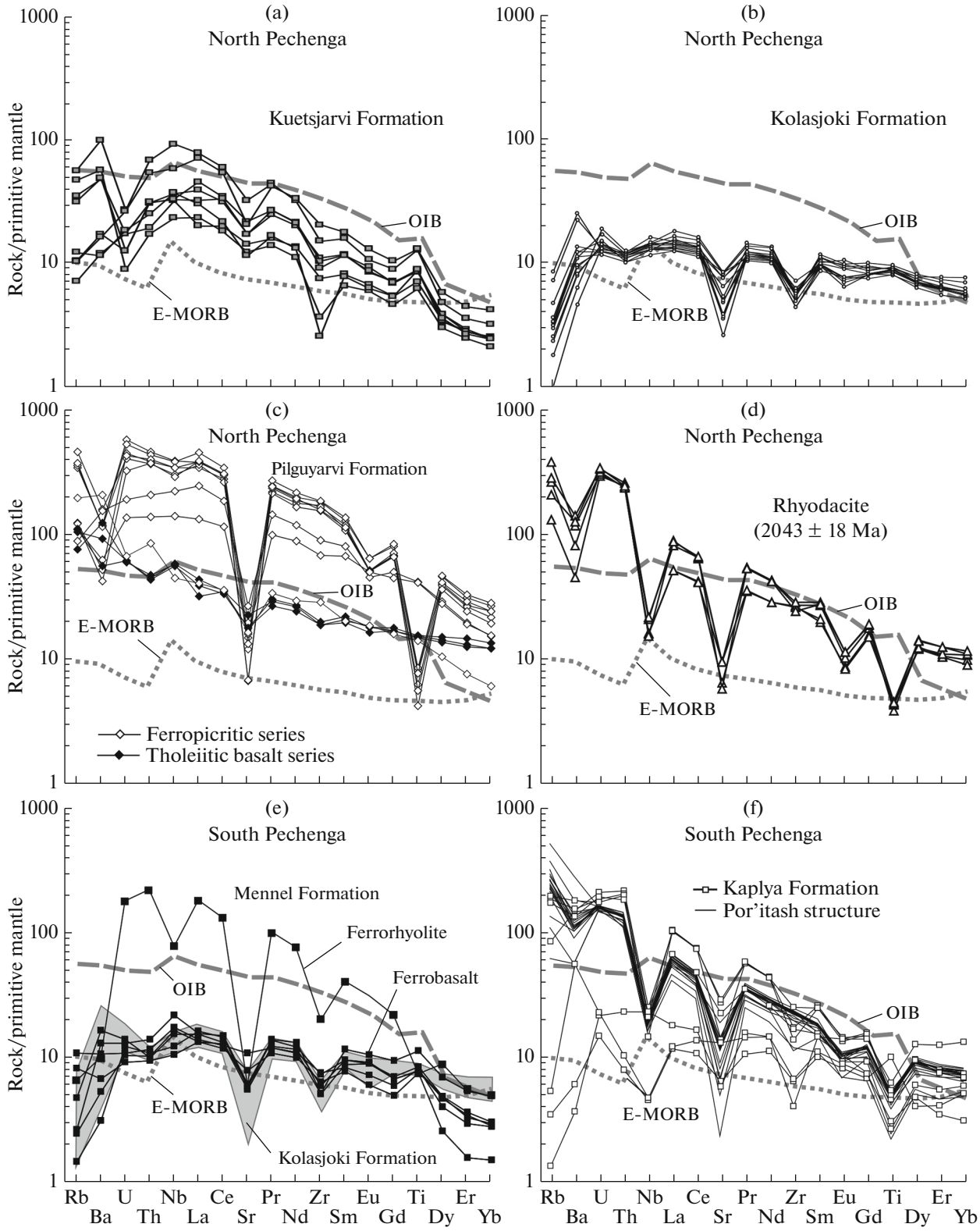

Fig. 6. Contents of trace elements in volcanic rocks of the (a) Kuetsjarvi, (b) Kolasjoki, and (c) Pilguyarvi formations, in rhyodacites from a sill from the Kola Superdeep Borehole (d), and in rocks of the Mennel Formation (e) and Kaplya Formation and Por'itash structure (f) normalized to primitive mantle. Hereinafter in Figs. 6, 8, 13–15, normalized factors and E-MORB and OIB values are given after (McDonough and Sun, 1995).

Table 2. Contents of major oxides (wt %) and trace elements (ppm) of representative samples of volcanic rocks from the Kuetsjarvi Formation of the Pechenga structure

Borehole	SX	SX	SX	SX	SX	SX	K-74	SX	SX	K-53	SG-3	SG-3
Depth, m	235.0	257.5	253.6	260.5	244.3	249.3	–	222.8	238.2	–	4757.9	4763.2
Rock	BA	BAA	BAA	BAA	BAA	BAA	MUD	ANBA	ANBA	DACI	RIOD	RIOD
SiO_2	47.95	52.70	52.06	47.40	51.85	52.55	49.31	53.94	54.22	61.03	70.87	68.09
TiO_2	1.09	1.54	1.50	2.22	1.50	2.29	2.56	1.26	1.58	1.29	0.75	0.78
Al_2O_3	7.06	10.52	11.15	13.16	11.68	12.15	14.35	10.89	10.56	9.20	12.79	14.83
Fe_2O_3	12.39	13.89	14.78	14.61	11.75	11.90	18.33	13.18	12.93	17.11	3.79	3.18
MnO	0.21	0.14	0.15	0.17	0.19	0.14	0.06	0.15	0.16	0.07	0.03	0.04
MgO	13.66	6.39	5.50	5.24	5.49	3.90	2.88	5.24	5.08	1.83	1.92	1.95
CaO	10.80	6.24	6.00	6.05	7.35	6.58	2.57	7.28	6.36	2.49	1.85	3.17
Na_2O	2.03	4.80	5.42	4.47	5.05	6.40	2.05	5.60	5.65	1.52	2.63	2.35
K_2O	1.27	0.81	0.25	1.61	0.41	0.37	4.47	0.34	0.87	2.76	2.43	2.72
P_2O_5	0.14	0.23	0.21	0.59	0.21	0.39	0.49	0.22	0.26	0.88	0.18	0.28
CO_2	1.38	1.11	1.26	1.70	2.02	1.74	0.03	0.79	0.84	0.11	0.40	0.54
S_{total}	0.02	0.02	0.02	0.02	0.03	0.01	0.00	0.01	0.00	0.07	0.11	0.13
LOI	2.83	2.09	2.12	3.24	2.68	1.63	2.82	1.25	1.90	2.24	1.92	2.12
Total	100.83	100.48	100.42	100.48	100.21	100.05	99.92	100.15	100.41	100.60	99.67	100.18
Li	12.1	9.15	7.32	22.6	11.3	7.31	29.8	2.52	8.06	14.0	31.8	40.2
Sc	27.9	20.3	20.7	12.8	17.3	13.2	22.3	19.3	20.3	20.3	22.2	23.3
V	233	274	304	337	297	270	322	241	247	31.1	47.7	51.0
Cr	1168	552	319	123	142	41	138	402	301	11.1	25.4	24.1
Co	53.6	57.1	45.6	39.5	38.8	27.2	35.6	38.0	41.4	20.7	6.87	6.04
Ni	184	215	102	105	60.1	31.5	105	108	94.9	15.5	17.7	17.9
Cu	80.1	31.0	260	105	50.7	65.0	164	65.1	50.3	173	7.32	9.62
Zn	105	96.7	90.1	122	125	87.6	92.8	75.5	88.1	115	50.0	48.0
Ga	11.4	13.2	15.0	18.1	16.4	13.3	33.7	12.5	14.0	14.8	21.7	24.3
Rb	25.2	18.9	3.8	30.2	5.6	5.6	111	6.6	16.9	86.1	137	149
Sr	226	261	314	589	397	376	103	211	314	36.9	169	168
Y	8.9	10.8	11.1	14.4	10.7	17.0	41.4	10.8	9.9	59.8	41.3	48.6
Zr	35.8	73.4	107	147	101	199	300	25.0	89.4	230	247	271
Nb	14.4	19.9	22.8	57.1	20.5	36.2	27.3	23.1	20.4	16.2	9.58	13.0
Ba	347	292	73.0	605	104	99.1	2929	70.2	297	413	485	834
La	14.5	12.4	24.1	48.1	28.2	43.9	43.1	18.5	20.0	37.1	30.7	48.7
Ce	29.2	32.0	50.5	96.0	55.6	87.3	91.4	35.0	53.7	80.8	65.0	102
Pr	3.40	3.86	6.02	10.8	6.50	10.2	11.5	4.04	6.51	10.4	8.5	12.9
Nd	13.3	16.2	24.1	38.4	25.6	40.1	50.7	15.8	25.4	46.4	33.0	49.6
Sm	2.55	3.17	4.57	6.15	4.52	6.92	12.0	3.05	4.52	11.1	7.86	10.8
Eu	0.87	0.98	1.23	1.56	1.36	1.91	2.98	0.92	1.27	2.56	1.19	1.61
Gd	2.37	2.80	3.66	4.61	3.56	5.38	10.7	2.78	3.59	10.9	7.50	9.38
Tb	0.36	0.44	0.51	0.68	0.52	0.78	1.55	0.40	0.52	1.82	1.25	1.49
Dy	1.92	2.16	2.48	3.07	2.47	3.72	7.72	2.20	2.30	10.1	7.59	8.88
Ho	0.38	0.43	0.47	0.58	0.46	0.74	1.39	0.43	0.44	2.10	1.45	1.78
Er	1.03	1.17	1.22	1.49	1.17	1.86	3.71	1.18	1.11	6.01	4.50	5.09
Tm	0.14	0.14	0.16	0.20	0.17	0.26	0.47	0.15	0.15	0.84	0.67	0.69
Yb	0.88	1.06	1.02	1.34	1.04	1.74	3.02	1.03	1.01	5.70	4.35	4.45
Lu	0.12	0.15	0.14	0.19	0.15	0.25	0.42	0.14	0.15	0.86	0.61	0.69
Hf	1.19	2.00	2.43	2.77	2.45	4.50	6.15	1.53	2.27	5.60	5.94	6.80
Ta	0.92	1.01	1.20	3.88	1.23	2.02	1.46	1.26	1.24	1.07	0.86	1.17
Pb	4.71	4.03	6.37	10.2	10.6	6.74	10.6	4.82	5.69	2.93	17.5	28.0
Th	1.40	1.58	2.52	5.56	2.50	4.41	6.32	2.04	2.55	4.86	18.6	20.7
U	0.18	0.35	0.36	0.55	0.26	0.54	0.91	0.38	0.26	1.67	6.34	6.68

Hereinafter in tables: LOI, loss on ignition; BA, basalt, FeBa, ferrobasalt, BAA, subalkaline basalt; MUD, mudgearite; AN, andesite; ANBA, basaltic andesite; DACI, dacite; RIOD, rhyodacite; FePi, ferropicrite; Pic, picrite; PicBa, picrobasalt.

Table 3. Contents of major oxides (wt %) and trace elements (ppm) of representative samples of volcanic rocks from the Kolasjoki Formation of the Pechenga structure

Borehole	S-41	S-41	S-41	S-41	S-41	S-41	S-41	S-41	S-41	S-41	S-41	S-41	S-41
Depth, m	39.0	40.0	80.6	81.8	120.5	89.0	89.8	133.7	133.1	243.0	243.5	274.7	274.5
Rock	FeBA	FeBA	FeBA	FeBA	FeBA	FeBA[1]	FeBA[2]	FeBA[1]	FeBA[2]	FeBA[1]	FeBA[2]	FeBA[1]	FeBA[2]
SiO_2	51.49	47.37	45.98	43.69	46.56	45.32	39.60	47.82	51.89	49.74	50.13	54.87	53.39
TiO_2	1.45	1.41	1.74	1.65	1.57	1.56	1.64	1.68	1.53	1.62	1.56	1.63	1.63
Al_2O_3	11.79	11.46	12.55	12.75	11.02	12.25	12.28	13.08	11.08	12.13	12.82	11.72	11.74
Fe_2O_3	14.54	12.94	16.92	19.82	15.42	13.81	20.92	15.57	13.00	15.54	15.85	11.93	15.69
MnO	0.20	0.18	0.19	0.22	0.21	0.19	0.23	0.19	0.17	0.18	0.20	0.17	0.17
MgO	5.93	5.43	8.36	9.70	5.90	7.33	9.77	7.00	6.53	4.92	4.75	4.19	4.72
CaO	6.97	10.98	7.96	6.88	10.68	8.90	9.04	6.39	7.62	7.11	6.26	9.10	8.11
Na_2O	4.04	2.89	1.84	1.86	2.34	3.58	0.84	3.21	3.98	4.18	4.33	2.59	2.39
K_2O	0.16	0.17	0.10	0.12	0.20	0.18	0.07	0.15	0.16	0.37	0.40	0.19	0.12
P_2O_5	0.09	0.09	0.12	0.11	0.15	0.10	0.08	0.16	0.13	0.12	0.12	0.15	0.12
CO_2	0.74	4.34	0.53	0.16	3.07	3.01	0.79	1.21	1.51	1.77	0.80	1.36	0.15
S_{total}	0.19	0.08	0.04	0.04	0.15	0.06	0.03	0.07	0.10	0.50	0.42	0.15	0.13
LOI	3.51	3.73	5.13	4.63	3.81	4.72	6.37	4.73	3.34	3.40	3.50	2.55	2.85
Total	101.10	101.07	101.46	101.63	101.08	101.01	101.66	101.26	101.04	101.58	101.14	100.60	101.21
Li	5.89	6.56	13.22	16.56	8.49	13.47	16.06	15.09	8.11	7.03	6.99	4.82	5.55
Sc	39.5	35.8	46.7	44.9	39.7	40.4	44.1	46.4	40.3	42.2	41.3	41.3	43.8
V	393	392	435	441	386	403	468	478	351	432	423	427	389
Cr	71.8	63.8	79.7	77.3	69.3	76.3	73.2	84.8	71.9	46.2	46.1	46.1	49.5
Co	47.3	38.9	48.8	50.5	46.9	45.6	44.8	53.8	38.2	52.7	53.1	42.8	46.4
Ni	57.5	51.4	59.9	66.3	54.2	58.8	58.6	70.0	50.7	62.6	61.7	58.5	59.9
Cu	148	149	143	123	153	162	127	189	154	241	179	189	139
Zn	106	95.2	127	140	116	104	137	125	96.7	119	125	89.7	112
Ga	11.8	13.1	16.3	16.9	11.2	14.1	19.3	17.9	11.4	14.5	14.5	12.1	13.2
Rb	1.76	1.83	0.96	1.37	2.61	1.97	0.53	1.60	1.71	4.05	4.79	1.80	1.26
Sr	90.2	122	156	99.2	159	91.8	145	71.0	46.9	66.7	67.0	143	160
Y	25.0	21.6	27.8	27.3	24.3	24.5	29.2	26.6	22.4	24.2	23.9	24.4	25.4
Zr	56.1	44.1	53.6	55.6	54.9	43.7	59.2	58.3	48.7	62.3	62.6	72.5	56.4
Nb	8.35	7.64	9.43	9.12	8.42	8.41	8.88	10.7	8.46	9.56	9.21	9.31	9.58
Ba	71.6	77.9	39.8	51.6	87.2	79.0	28.6	61.4	58.9	147	165	70.5	50.8
La	10.2	8.18	10.8	9.92	8.54	8.24	8.60	9.78	8.89	9.33	9.12	9.43	11.9
Ce	22.7	19.1	26.0	24.1	20.4	19.9	20.8	23.1	21.3	22.5	21.9	22.7	27.6
Pr	3.04	2.65	3.51	3.41	2.81	2.74	2.92	3.15	2.93	3.03	3.05	3.16	3.71
Nd	13.8	12.5	16.7	15.6	13.2	12.9	13.7	14.6	13.4	14.1	13.8	14.1	17.0
Sm	3.85	3.49	4.78	4.50	3.98	3.76	4.10	4.21	3.85	3.99	3.90	4.01	4.55
Eu	1.15	1.16	1.51	1.39	1.06	1.12	1.62	1.49	0.96	1.15	1.16	1.37	1.44
Gd	4.38	4.01	5.38	4.96	4.28	4.27	4.76	4.64	4.28	4.38	4.40	4.37	5.07
Tb	0.75	0.68	0.91	0.87	0.74	0.75	0.81	0.81	0.75	0.77	0.78	0.76	0.83
Dy	4.39	4.15	5.39	5.16	4.58	4.57	5.17	4.87	4.57	4.68	4.54	4.61	4.94
Ho	0.89	0.86	1.13	1.09	0.98	0.97	1.10	1.01	0.91	0.98	0.95	0.95	1.01
Er	2.64	2.37	3.17	3.00	2.77	2.71	3.33	2.80	2.64	2.71	2.61	2.65	2.70
Tm	0.36	0.34	0.43	0.44	0.38	0.38	0.50	0.37	0.40	0.36	0.36	0.37	0.38
Yb	2.33	2.20	2.99	2.68	2.52	2.51	3.30	2.51	2.32	2.54	2.36	2.41	2.51
Lu	0.31	0.28	0.41	0.37	0.36	0.35	0.44	0.36	0.33	0.34	0.36	0.33	0.37
Hf	1.87	1.71	2.16	1.92	1.79	1.80	1.99	2.15	2.01	2.07	2.01	1.93	2.08
Ta	0.64	0.59	0.75	0.64	0.57	0.58	0.63	3.41	0.57	0.99	0.84	0.60	0.73
Pb	1.67	1.19	1.21	1.06	1.00	0.97	0.96	0.98	0.96	0.99	1.31	1.22	1.17
Th	0.87	0.87	1.07	0.98	0.98	0.94	0.98	1.05	0.94	1.02	0.98	1.01	1.03
U	0.25	0.33	0.41	0.31	0.27	0.27	0.30	0.28	0.29	0.28	0.27	0.38	0.31

Pillow lava: [1]center; [2]rim.

Table 4. Contents of major oxides (wt %) and trace elements (ppm) of representative samples of volcanic rocks from the Pilguyarvi Formation of the Pechenga structure

Borehole	S-91/ IV-1	S-91/ IV-2	S-91/ IV-3	S-91/ IV	S-87	S-89	S-87	S-89	S-89	S-89	S-89	S-89
Depth, m	–	–	–	400	19	212	23	202	205	207	209	216
Rock	FeBa[1]	FeBa1	FeBa1	FePi[1]	FeBa[2]	FeBa[2]	FeRi[2]	FeRi[2]	FeRi[2]	FeRi[2]	FeRi[2]	FeRi[2]
SiO_2	48.59	49.50	50.25	45.82	49.36	46.44	74.95	72.26	77.09	71.15	76.58	72.54
TiO_2	0.95	1.00	1.01	0.85	2.60	2.69	0.41	0.54	0.38	0.56	0.28	0.51
Al_2O_3	12.76	13.62	14.08	4.98	11.79	11.70	10.31	10.39	8.38	10.84	9.46	10.67
Fe_2O_3	11.63	11.19	11.91	17.48	11.83	15.05	5.26	7.24	5.85	7.29	4.77	6.16
MnO	0.17	0.15	0.17	0.19	0.15	0.18	0.05	0.10	0.06	0.10	0.07	0.10
MgO	7.19	7.16	7.60	15.86	5.77	5.85	1.06	0.69	1.44	0.73	0.80	0.89
CaO	11.31	11.62	8.88	3.37	7.20	10.65	0.59	0.83	0.41	0.94	0.73	1.50
Na_2O	1.80	2.06	2.91	0.57	1.96	2.98	4.46	3.23	1.78	4.29	1.77	3.23
K_2O	0.88	0.57	0.58	0.80	0.97	0.91	1.11	3.27	3.39	2.60	4.25	3.30
P_2O_5	0.09	0.14	0.10	0.16	0.43	0.32	0.05	0.04	0.04	0.07	0.05	0.04
CO_2	1.99	0.85	0.19	1.96	3.20	0.01	0.17	0.02	0.16	0.06	0.06	0.13
S_{total}	0.00	0.00	0.03	0.21	0.02	0.03	0.33	0.24	0.03	0.28	0.05	0.02
LOI	3.49	3.12	2.82	7.60	4.20	3.56	1.50	1.36	1.17	1.51	1.13	1.24
Total	100.85	100.98	100.53	99.85	99.48	100.37	100.25	100.21	100.18	100.42	100.00	100.33
Li	12.9	11.0	9.05	8.05	18.0	8.45	8.83	3.27	4.73	3.76	3.45	3.16
Sc	37.8	39.0	39.0	11.6	17.6	37.1	6.39	7.57	8.12	7.59	7.13	9.38
V	271	282	271	145	226	416	5.38	22.1	30.9	19.8	7.34	29.3
Cr	128	132	135	264	185	226	31.3	65.7	89.6	60.8	69.6	69.3
Co	43.5	45.2	46.5	103	43.5	49.8	3.40	7.48	8.37	6.39	3.62	6.61
Ni	96.8	97.8	103	735	176	124	22.3	37.7	56.3	33.6	22.5	27.8
Cu	119	133	128	379	57.6	190	16.5	24.4	35.2	31.9	21.4	27.3
Zn	77.9	73.9	78.9	112	137	126	81.6	203	152	216	150	176
Ga	12.6	13.7	14.4	9.05	21.4	26.8	29.3	31.0	15.5	26.9	23.4	27.8
Rb	21.0	21.8	15.1	39.3	17.8	22.0	24.6	68.1	74.6	71.2	91.2	75.0
Sr	120	152	120	111	181	108	45.2	81.1	70.3	100	89.8	132.8
Y	17.1	17.8	18.4	11.3	30.4	28.6	44.4	49.4	31.7	55.2	43.9	46.1
Zr	68.3	68.2	72.3	104	325	245	619	664	581	675	557	602
Nb	12.8	13.5	13.2	10.3	50.9	32.5	78.7	89.5	67.9	88.7	69.9	78.7
Ba	208	126	279	471	349	141	117	267	363	268	358	261
La	8.90	9.94	7.34	9.20	56.0	30.4	78.8	86.3	19.1	103.6	83.3	88.4
Ce	19.8	21.1	20.8	21.4	110.2	68.6	166.0	181.7	63.4	204.9	157.0	177.2
Pr	2.42	2.61	2.72	3.02	13.0	9.0	19.9	22.3	9.6	24.5	19.3	21.3
Nd	10.7	11.6	12.0	12.9	52.8	39.1	78.4	88.4	41.9	95.5	73.7	83.5
Sm	2.82	2.97	3.16	2.89	11.52	9.65	15.9	18.5	11.8	19.6	15.6	17.0
Eu	0.88	0.98	0.98	1.00	2.45	2.72	2.79	3.49	1.60	3.48	2.76	2.78
Gd	3.21	3.20	3.41	3.04	9.47	8.52	13.0	15.3	10.0	15.9	12.7	13.6
Tb	0.54	0.53	0.59	0.47	1.35	1.31	2.03	2.41	1.68	2.45	1.98	2.09
Dy	3.22	3.40	3.59	2.50	6.87	6.56	9.46	10.9	7.78	11.1	9.17	9.69
Ho	0.67	0.73	0.73	0.44	1.18	1.20	1.66	1.92	1.37	2.06	1.63	1.71
Er	1.94	2.04	2.25	1.17	3.05	2.96	4.20	4.85	3.26	5.07	4.06	4.49
Tm	0.26	0.28	0.30	0.16	0.36	0.41	0.54	0.65	0.44	0.70	0.54	0.58
Yb	1.88	1.88	2.06	0.94	2.36	2.38	3.74	4.12	2.68	4.33	3.32	3.74
Lu	0.27	0.30	0.32	0.13	0.33	0.32	0.46	0.51	0.36	0.53	0.44	0.49
Hf	1.84	1.84	2.07	2.78	7.43	6.27	13.1	15.0	12.9	14.4	12.2	13.2
Ta	0.68	0.73	0.96	0.68	2.70	1.84	3.92	4.74	3.55	4.40	3.41	3.95
Pb	1.58	1.79	1.15	3.28	6.21	2.61	19.3	18.4	16.5	12.5	14.8	17.0
Th	1.31	1.36	1.42	2.56	6.30	4.18	11.7	13.9	11.5	13.3	11.2	12.2
U	0.47	0.46	0.46	0.50	1.45	1.04	3.39	4.38	2.92	4.02	3.05	3.23

[1]Upper part of the section; [2]lower part of the section.

ies of this formation have moderate TiO_2 and Fe_2O_{3total} contents (Fig. 5) in comparison with Pilguyarvi analogs. At the same time, the Mennel rocks have negative Sr and Zr anomalies and no Nb anomaly, similar to Kolasjoki volcanic rocks. The Mennel ferrobasalts exhibit more fractionated HREE patterns ($(Gd/Yb)_N$ = 0.9–3.2) and no Eu anomaly (Eu/Eu* = 0.90–1.09).

The Kaplya volcanic rocks include the basalt–andesite–dacite–rhyolite association with dominant felsic and intermediate rocks characterized by high alkali sum and low Ti content and Fe# value. Their geochemical features are widely variable and most varieties have evident negative Nb anomaly (Nb/Nb* ~ 0.35).

The salic subalkali basaltic andesites, andesites, and dacites are dominant amid the volcanic rocks of the Por'itash Fault. These rocks, which are geochemically similar to the latest derivates of the Kaplya Formation (Skuf'in, 2018a), are strongly enriched in LILEs, HSFEs, and REEs, similar to the Pilguyarvi ferrorhyolites.

Volcanic Rocks of the Imandra–Varzuga Structure

The Umba volcanic rocks form the picrobasalt–trachybasalt–trachyandesite–trachydacite series with dominant mafic varieties (Table 6). Picrites are low-Fe (Fe_2O_{3total} < 15 wt %) and moderately Ti (TiO_2 < 1.4 wt %). The basalts are subalkali ($Na_2O + K_2O$ ~ 5 wt %, $Na_2O > K_2O$) (Fig. 7). The Fe trachyandesites (55–56 wt % SiO_2 on average) have higher Fe_2O_{3total} content and alkali sum (12.68 and 7.9 wt %, respectively). Scarce contents of trace elements (Mints et al., 1996) allow their classification as OIBs with low contents of Ni (30–40 ppm), Cu (20–60 ppm), and Cr (100–150 ppm).

The Ilmozero tholeiitic lavas include more evolved (relative to the Kolasjoki analogs) basaltic andesite–andesite–dacite series with no mafic members, higher alkali contents (first of all, K_2O), and lower Ti and Fe contents (Fig. 7, Table 6). The pattern of trace elements in these basalts also differs from those of the Pechenga tholeiites. In particular, the Ilmozero basalts exhibit higher LILE and HSFE contents, more fractionated REE patterns ($(La/Yb)_N$ = 7.1–8.7), and negative Nb anomaly (Nb/Nb* ~ 0.30) along with Sr and Zr minima.

The Tominga volcanic rocks are rather similar in composition of major oxides to the Pilguyarvi analogs of the Pechenga structure; however, they have minor varieties with MgO contents of >9 wt % (Fig. 7). The pattern of trace elements indicates the presence of two groups among basalts. Group 1 with minor negative Zr anomaly and low partition coefficient of both LREEs and HREEs ($(La/Yb)_N$ = 0.62–0.89) is moderately rich in trace elements and are similar to those of the Kolasjoki Formation (Fig. 8). The rocks of group 2 with strong enrichment in LILEs, HSFEs, and REEs, negative Sr anomaly (Sr/Sr* ~ 0.16), negative Ba and Ti anomalies in ferrorhyolites, more fractionated LREE ($(La/Sm)_N$ = 3.7–4.6) and HREE ($(Gd/Yb)_N$ = 3.3–3.6) patterns, and the lack of Eu anomaly (Eu/Eu* = 0.90–1.06) are geochemically similar to the Pechenga ferropicrites.

The volcanic rocks of the Pechenga caldera are part of a volcano-plutonic association and belong to the subalkaline monzonite–trachyandesite series with typically dominant salic derivatives and higher contents of incoherent elements typical of those of OIBs (Fig. 8c). There is a regular increase in contents of most trace elements from basalts to trachyandesites, rhyolites, and monzonites. The most alkaline members of the series are geochemically similar to the rocks of the Soustov complex (Bea et al., 2001), which is also located within the Tominga Formation, west of the Panarechka structure (Fig. 4). Rare basalts are characterized by negative Ti and Nb anomalies (Nb/Nb* = 0.1–0.8) (Fig. 8) and change of positive Sr and negative Zr anomalies and vice versa within the basalt–trachyandesite–monzonite series.

GEOCHRONOLOGY AND GEOCHEMISTRY OF SUBVOLCANIC ROCKS

The mafic dikes and sills with age of 2.06–1.86 Ga are discussed on the basis of new original geochronological and geochemical data and published results.

U–Pb Geochronology and Sm–Nd Isotopic Geochemistry

Baddeleyite from a gabbronorite dike (Sample Sa-539-5) forms platy and pseudoprismatic, transparent, rarely semitransparent brown and dark brown crystals with a homogeneous internal structure and smooth surfaces. The U–Pb age was obtained for one grain 50–60 μm in size and two microsamplings (8–10 most transparent baddeleyite crystals with size of 30–40 μm) (Table 7). This baddeleyite is characterized by minor age discordance (<1%) or is concordant (Table 7, no. 3). The points of isotopic composition are approximated by a discordia (Fig. 9), the upper intersection of which with concordia corresponds to the age of 1981 ± 4 Ma (MSWD = 0.02), whereas the lower intersection corresponds to the age of 390 ± 460 Ma. The concordant age of eight dark brown crystals of 1983 ± 5 Ma (MSWD = 0.47, probability = 0.49) coincides with the age determined by the upper intersection of discordia and average age calculated from $^{207}Pb/^{206}Pb$ ratio for baddeleyite (1981 ± 3 Ma, MSWD = 0.64). The latter can be considered as the most precise estimate of the age of crystallization of parental melts for gabbronorites.

The zircon grains extracted from a ferropicrite dike exhibit unusual platy morphology without crystal habitus. The BSE (Fig. 10) and CL (Fig. 11) images shows that this morphology is a result of pseudomorphic

Table 5. Contents of major oxides (wt %) and trace elements (ppm) of representative samples of volcanic rocks from the southern part of the Pechenga structure

Formation	MEN	MEN	MEN	MEN	KAP	KAP	KAP	KAP	KAP	POR	POR	POR
Rock	Pic	PicBa	BA	Pic	ANBA	AN	ANBA	AN	AN	DACI	AN	AN
SiO_2	44.51	47.52	46.49	45.67	54.66	56.30	56.39	56.54	57.58	63.08	61.38	60.69
TiO_2	1.85	2.23	2.13	1.09	0.57	1.81	0.86	0.93	1.02	0.91	0.94	0.98
Al_2O_3	7.29	9.89	11.15	6.98	15.25	13.41	13.80	14.77	15.52	14.34	14.65	14.93
Fe_2O_3	13.69	14.84	12.43	13.41	7.53	14.87	6.71	9.32	8.06	7.46	8.10	7.69
MnO	0.19	0.15	0.19	0.19	0.09	0.16	0.09	0.09	0.08	0.07	0.09	0.07
MgO	18.02	12.75	8.21	18.40	5.39	4.44	6.79	4.89	4.04	2.50	2.78	2.36
CaO	7.89	4.33	7.24	7.68	6.18	0.46	6.36	3.69	3.60	3.44	3.61	4.44
Na_2O	0.49	2.45	3.01	0.65	4.97	2.84	4.14	4.07	4.24	2.31	2.76	2.53
K_2O	0.03	0.17	0.92	0.05	2.19	0.09	2.28	3.24	3.40	3.28	2.69	3.12
P_2O_5	0.12	0.18	0.20	0.10	0.32	0.24	0.32	0.32	0.35	0.19	0.17	0.18
CO_2	1.07	1.21	5.24	0.47	0.50	0.01	0.23	0.54	0.86	0.09	0.05	0.02
S_{total}	0.08	0.05	0.01	0.17	0.06	0.01	0.02	0.01	0.01	0.04	0.03	0.08
LOI	5.44	4.34	3.39	6.13	2.49	6.17	2.22	1.86	1.79	2.60	3.00	2.99
Total	100.67	100.11	100.61	100.99	100.20	100.81	100.21	100.27	100.55	100.31	100.25	100.08
Li	15.7	25.5	4.44	7.36	14.3	35.4	12.0	23.8	19.7	26.2	26.7	19.1
Sc	24.6	24.9	22.9	18.7	37.5	45.9	19.0	21.8	22.8	23.4	27.2	29.4
V	220	189	213	49.9	222	296	112	125	131	146	163	183
Cr	1156	1168	662	1611	1033	15.3	189	191	198	75.9	86.4	103
Co	68.8	70.2	47.6	66.8	60.6	32.0	20.1	29.3	29.3	21.0	19.8	22.3
Ni	600	681	407	634	349	15.5	81.1	97.4	101	35.2	33.2	40.7
Cu	36.8	38.4	14.1	15.0	40.1	48.3	12.4	51.8	51.3	31.7	28.8	51.9
Zn	94.3	92.0	64.8	63.8	78.2	124	64.0	103	115	83.9	93.0	93.9
Ga	11.6	12.3	4.99	5.56	9.07	18.3	14.7	19.2	19.0	20.8	22.9	25.3
Rb	5.77	2.54	0.79	0.39	0.75	1.96	48.0	105	112	139	111	126
Sr	196	108	106	53.6	112	123	267	528	558	215	221	271
Y	12.6	11.2	12.7	7.38	13.2	14.8	30.8	32.4	31.5	33.1	34.5	34.2
Zr	49.6	72.5	70.5	49.6	68.1	65.5	177	143	261	207	224	233
Nb	10.7	9.43	7.55	3.47	15.1	2.93	16.5	14.4	9.54	11.8	12.3	14.0
Ba	64.5	99.7	18.8	13.1	23.3	38.7	967	1000	1160	759	574	731
La	8.50	9.43	10.0	1.92	11.7	7.59	66.5	68.2	67.1	37.9	39.0	41.3
Ce	19.8	21.1	23.2	8.01	28.2	18.3	128	128	125	71.3	73.7	78.4
Pr	2.87	2.89	3.29	0.66	4.02	2.73	14.8	14.6	14.9	8.93	9.04	9.67
Nd	13.0	12.7	14.4	3.36	18.5	14.1	55.7	54.6	54.7	34.8	35.9	36.3
Sm	3.38	3.21	3.66	1.11	4.53	4.10	10.6	10.1	10.2	7.25	7.55	7.45
Eu	1.29	1.05	1.33	0.34	1.35	1.25	2.15	2.22	2.07	1.60	1.52	1.59
Gd	3.44	3.05	3.43	1.26	3.98	3.65	8.49	8.05	8.26	6.28	6.33	6.18
Tb	0.56	0.51	0.58	0.26	0.68	0.54	1.34	1.31	1.31	1.03	1.05	1.04
Dy	3.00	2.58	3.05	1.46	3.22	2.72	6.44	6.33	6.39	6.01	6.16	6.05
Ho	0.57	0.48	0.57	0.32	0.60	0.57	1.27	1.25	1.24	1.25	1.25	1.21
Er	1.43	1.24	1.38	0.92	1.53	1.81	3.46	3.32	3.27	3.55	3.62	3.52
Tm	0.19	0.18	0.20	0.13	0.20	0.30	0.50	0.47	0.45	0.47	0.49	0.49
Yb	1.17	1.16	1.22	1.00	1.35	2.25	3.23	2.96	2.99	3.20	3.36	3.18
Lu	0.17	0.13	0.16	0.14	0.16	0.35	0.40	0.36	0.38	0.47	0.51	0.50
Hf	1.40	2.09	2.16	1.48	2.03	1.83	4.71	3.38	6.01	5.53	5.80	5.80
Ta	0.98	0.77	0.71	0.30	1.29	0.30	1.26	1.04	0.82	0.93	0.94	0.99
Pb	4.03	1.67	1.50	1.14	2.44	3.63	9.28	17.8	18.8	19.1	12.9	12.4
Th	0.94	0.81	0.88	1.50	1.98	0.68	18.8	17.8	17.3	11.6	11.5	11.6
U	0.22	0.28	0.25	0.38	0.46	0.32	4.53	4.03	3.78	3.46	3.35	3.22

MEN, Mennel Formation of the Braginsky volcanic center; KAP, Kaplya Formation (area of Lake Poroyarvi); POR, volcanic rocks of the Por'itash Fault.

Table 6. Contents of major oxides (wt %) and trace elements (ppm) of representative samples of volcanic rocks from the Imandra–Varzuga structure

Area	PANA	PANA	PANA	PANA	PANA	ILM	ILM	TOM	TOM	TOM	TOM	TOM
Borehole	PN-1	PN-1A	P -4	S-07/14	SP-07/01A	S-07/30	S-07/32	STP-07	VLC-7	VLC-8	VLC-9	VLC-10
Rock	MON	MON	TAN	BA	PRD	BA	BA	BA	BA	BA	BA	BA
SiO_2	64.53	65.62	57.64	50.63	38.48	54.60	53.94	47.19	50.80	51.30	51.04	54.95
TiO_2	0.79	0.65	0.54	0.89	0.10	0.83	0.81	1.49	2.49	2.94	2.84	2.68
Al_2O_3	14.80	16.27	19.08	13.53	2.04	13.25	13.47	13.25	18.87	18.29	18.58	17.28
Fe_2O_3	4.05	3.01	5.12	15.06	9.32	10.56	11.04	14.94	9.64	8.83	8.62	9.24
MnO	0.08	0.07	0.07	0.24	0.15	0.15	0.16	0.25	0.10	0.10	0.11	0.08
MgO	1.90	1.17	2.44	5.76	30.72	6.16	6.22	6.56	4.35	3.31	3.10	3.83
CaO	2.53	1.32	5.63	8.38	2.89	8.08	6.79	9.08	2.59	3.30	3.74	2.30
Na_2O	4.18	4.35	3.99	2.03	0.04	1.94	2.22	1.75	5.93	4.68	5.40	3.39
K_2O	3.81	5.20	0.98	1.31	0.01	1.89	1.43	1.37	0.64	1.72	1.27	1.69
P_2O_5	0.17	0.13	0.09	0.09	0.01	0.10	0.10	0.10	0.73	0.66	0.56	0.68
CO_2	1.27	0.42	1.73	–	–	–	–	–	0.72	1.65	1.69	0.94
S_{total}	0.04	0.05	0.13	0.17	0.12	0.03	0.05	0.03	–	–	–	–
LOI	1.71	1.35	3.21	3.07	15.32	2.08	3.41	3.55	3.68	3.92	3.45	3.31
Total	99.86	99.61	100.65	101.16	99.20	99.67	99.64	99.56	100.54	100.70	100.40	100.37
Li	17.7	16.1	15.8	12.9	0.32	7.71	14.7	6.78	5.57	5.49	5.42	6.30
Sc	8.40	5.30	25.1	48.1	10.7	28.9	27.1	51.7	4.18	5.57	5.15	4.09
V	69.1	54.3	171.7	391	34.2	205	203	437	24.9	52.1	43.0	40.6
Cr	54.8	34.0	37.2	86.6	4302	327	262	72.7	4.74	8.50	3.26	5.53
Co	11.3	6.3	15.4	51.2	121	39.9	39.6	47.4	16.3	16.3	14.3	15.2
Ni	36.9	25.7	18.7	65.6	2010	110.9	104.7	74.2	2.73	4.71	4.24	3.43
Cu	33.0	11.6	43.2	115.2	20.4	115.1	93.1	132.3	10.7	14.9	10.2	9.6
Zn	132	82.5	67.7	122	60.0	80.9	83.3	137.0	155	184	204	151
Ga	18.2	22.0	15.6	14.4	2.48	17.2	17.4	19.5	27.1	27.0	26.9	24.6
Rb	138	92.7	18.9	39.7	0.96	46.7	55.5	10.9	13.0	37.9	28.9	28.6
Sr	314	294	244	133	73.7	293	245	355	137	155	152	119
Y	17.8	16.7	11.5	26.6	1.81	17.0	16.2	24.3	29.4	25.7	27.4	24.8
Zr	271	297	41.2	33.9	4.17	95.6	95.4	61.7	346	297	362	326
Nb	17.7	17.5	3.52	1.85	0.69	6.29	5.86	8.28	98.6	93.1	130	89.5
Ba	782	1107	180	291	11.8	508	323	640	297	591	491	593
La	46.2	45.4	9.76	2.92	0.37	20.4	15.2	9.51	87.1	76.6	85.5	60.4
Ce	85.5	62.6	18.9	8.93	0.67	40.5	39.6	18.5	175	160	174	136
Pr	9.83	9.93	2.55	1.29	0.09	4.93	4.73	2.93	20.6	18.5	20.4	14.9
Nd	34.8	33.5	10.7	6.49	0.33	19.0	18.3	13.2	75.1	71.6	74.3	55.6
Sm	5.67	5.50	2.45	2.05	0.12	4.09	3.80	4.13	13.8	12.6	13.5	10.1
Eu	1.14	1.24	0.70	0.79	0.07	1.04	1.01	1.33	3.50	3.69	3.92	3.14
Gd	4.45	4.24	2.24	2.89	0.19	3.63	3.48	4.53	10.4	9.48	10.2	8.09
Tb	0.69	0.68	0.37	0.60	0.04	0.58	0.55	0.78	1.31	1.24	1.38	1.17
Dy	3.65	3.61	2.09	4.08	0.32	3.26	3.02	4.97	6.55	6.08	6.64	5.86
Ho	0.74	0.73	0.45	0.96	0.08	0.63	0.59	1.03	1.18	1.08	1.17	1.09
Er	2.20	2.08	1.26	3.03	0.23	1.80	1.69	2.95	2.87	2.64	2.83	2.36
Tm	0.33	0.30	0.20	0.45	0.04	0.25	0.23	0.40	0.41	0.35	0.39	0.35
Yb	2.21	1.97	1.20	3.22	0.20	1.59	1.46	2.58	2.36	2.13	2.30	2.00
Lu	0.32	0.32	0.16	0.46	0.03	0.21	0.22	0.36	0.32	0.27	0.30	0.26
Hf	6.87	7.87	1.16	1.06	0.13	2.40	2.39	1.79	8.13	7.32	8.11	7.32
Ta	1.09	1.19	0.32	0.21	0.12	0.51	0.48	0.62	7.72	7.47	7.51	6.44
Pb	36.6	40.0	5.98	4.88	0.66	4.07	4.02	4.91	6.69	5.68	4.70	4.49
Th	22.2	26.1	2.87	0.38	0.10	3.69	3.37	0.81	10.2	9.12	9.80	6.80
U	3.47	2.52	1.38	0.21	0.03	0.87	0.79	0.20	1.96	1.69	1.61	1.35

MON, monzonite; TAN, trachyandesite; PRD, peridotite; PANA, Panarechka structure; TOM, Tominga Formation; ILM, Ilmozero Formation. For other notation, see Table 5.

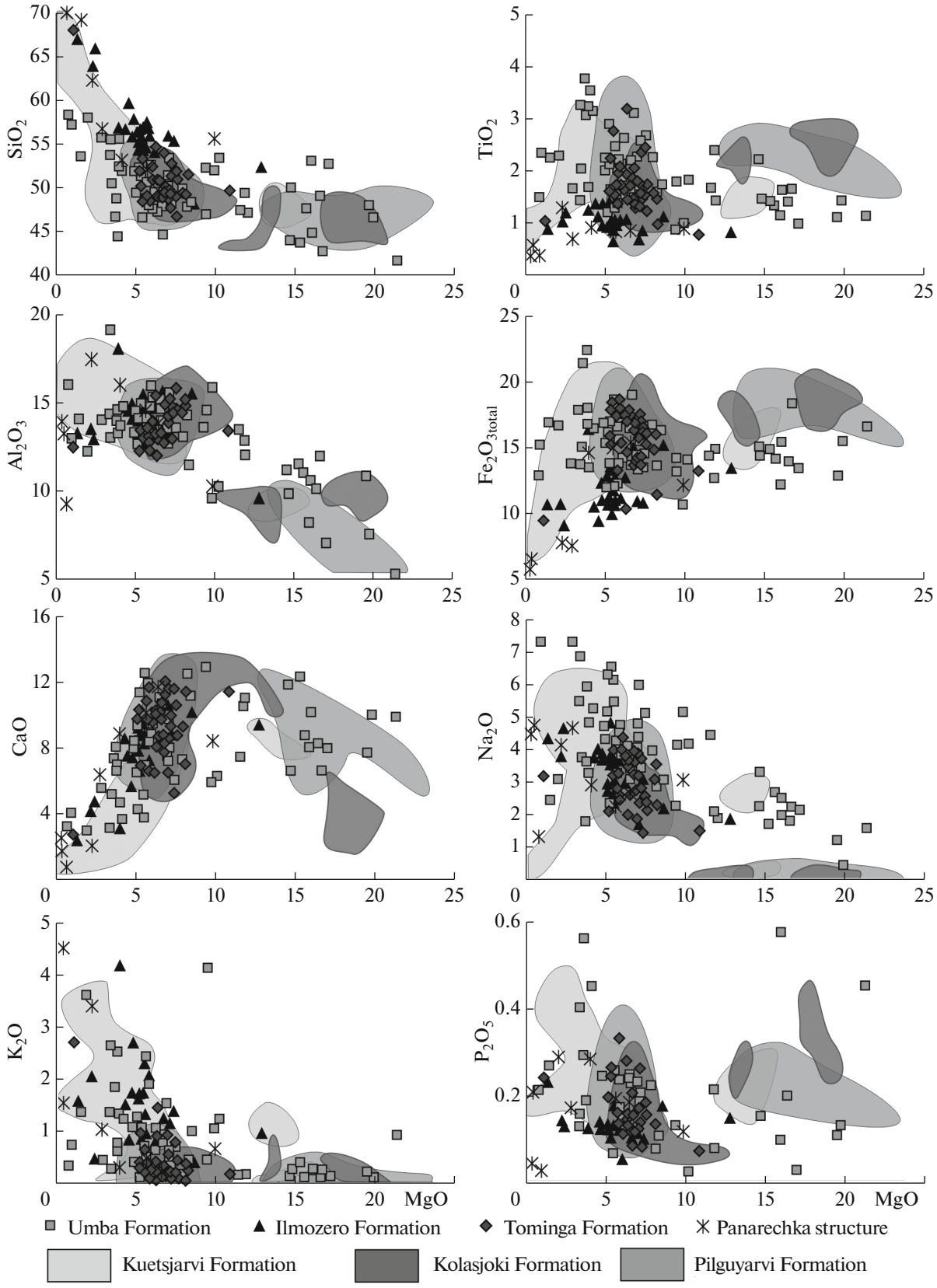

Fig. 7. MgO–oxide plot (wt %) for the Early Proterozoic volcanic rocks of the Imandra–Varzuga structure on the basis of original and published data (Fedotov, 1985; Predovskii et al., 1974; Smolkin, 1992; Zagorodny et al., 1982). Fields show the composition of rocks of the Kuetsjarvi, Kolasjoki, and Pilguyarvi formations of the Pechenga structure.

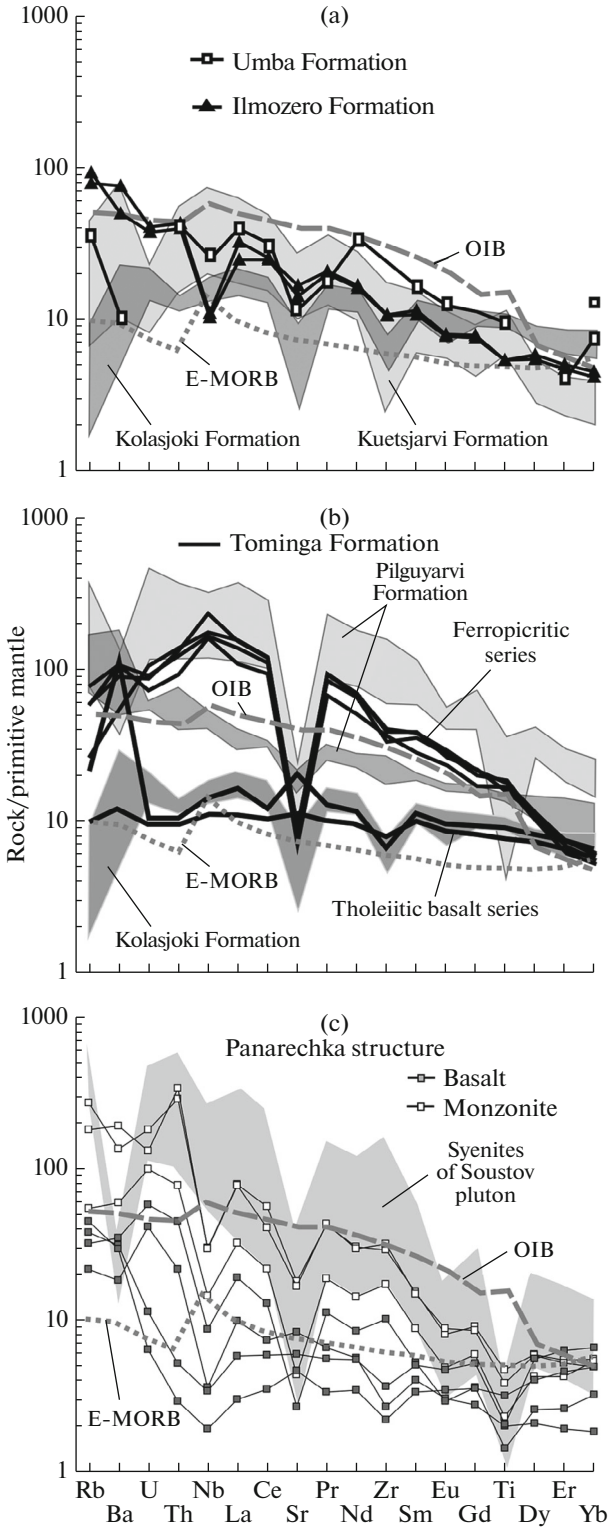

Fig. 8. Contents of trace elements in volcanic rocks of the (a) Umba and Ilmozero and (b) Tominga formations and (c) Panarechka structure of the Imandra–Varzuga zone normalized to primitive mantle. Fields show the composition of rocks of the Kuetsjarvi, Kolasjoki, and Pilguyarvi formations of the Pechenga structure and syenites of Soustov pluton after (Bea et al., 2001). The data on the Umba Formation are after (Mints et al., 1996).

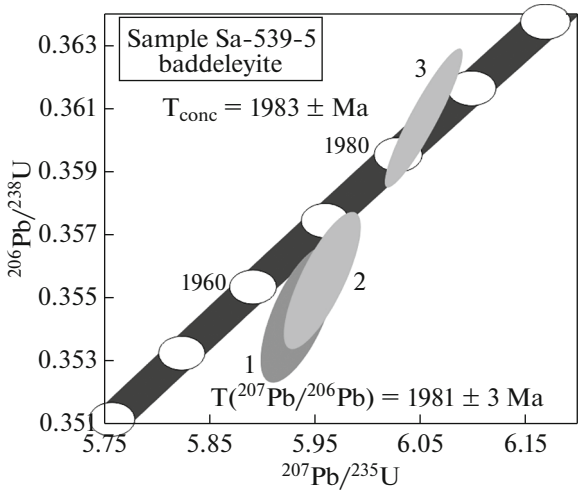

Fig. 9. Plot with concordia for baddeleyite from a gabbronorite dike (Sample Sa-539-5). Numbers of points correspond to those in Table 7.

replacement of primary igneous baddeleyite, the relics of which are identified by means of a microprobe.

The U–Pb isotopic study of platy zircon grains has revealed another degree of discordance, which is approximated by one line, the upper and lower intersections of which with concordia correspond to the age of 1786 ± 14 and 362 ± 70 Ma, respectively (Fig. 11b). The age of relict baddeleyite estimated from the $^{207}Pb/^{206}Pb$ ratio is ~1970 Ma (Fig. 11c). Thus, the age of zircon from ferropicrite (1786 ± 14 Ma) is interpreted as the age of metamorphism of rock, whereas the disturbance of the zircon isotopic system at ~360 Ma probably reflects the influence of the Devonian magmatic event largely manifested on the Kola Peninsula. Owing to an insufficient amount of material, the age of 1970 Ma of relict baddeleyite can only approximately reflect the time of crystallization of ferropicrite.

According to (Galimzyanova et al., 2006; Hanski, 1992; Hanski et al., 2014; Skuf'in and Bayanova, 2006; Smolkin, 2014), the Nd isotopic characteristics of mafic dikes of the Murmansk Terrane (Table 8) and compared volcanic rocks from Pechenga and Imandra–Varzuga structures demonstrate a significant range of $\varepsilon_{Nd}(T)$ values (from +3.9 to –7.1), which is evidently caused by a different fraction of ancient crustal matter in their composition. The maximum negative $\varepsilon_{Nd}(T)$ values of the Kuetsjarvi rocks reflect the contribution of continental sediments during intrusion of mafic melts under subaerial conditions. The $\varepsilon_{Nd}(T)$ values of +1.7 for the Kirkenes metadolerites with age of 2.06 Ga indicate similar isotopic composition of the entire series of mafic melts of the Kuetsjairvi Formation and later Kolasjoki and Pilguyarvi tholeiitic volcanic rocks. The positive $\varepsilon_{Nd}(T)$ values corrected for the age of 1983 Ma are determined

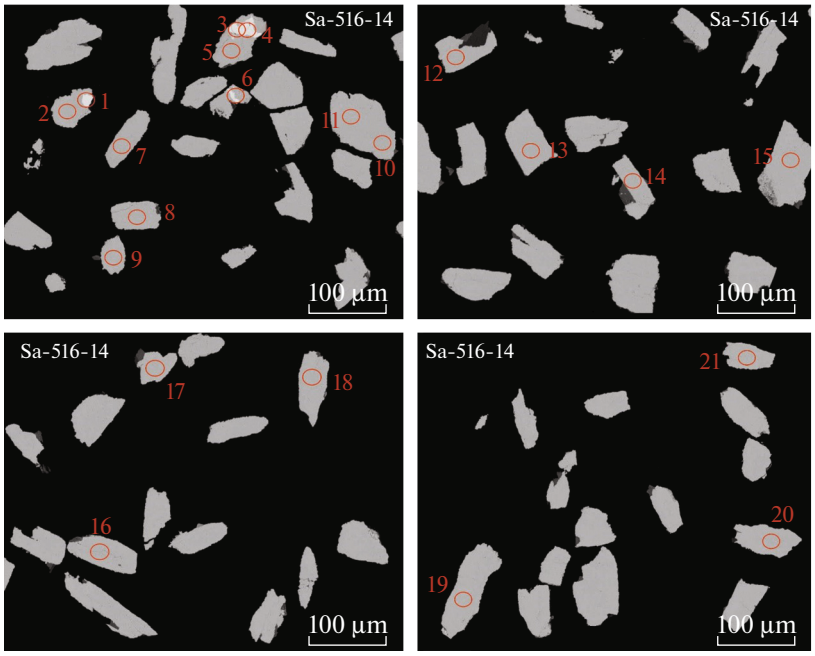

Fig. 10. BSE images of zircons from metamorphosed ferropicrite (Sample Sa-516-14). The points indicate the areas of local U–Pb analyses.

Table 7. Results of U–Pb isotopic studies of baddeleyite from ferrodolerite (Sample Sa-539-5)

No.	Fraction (μm) and characteristic of baddeleyite	U/Pb*	Pb_c/Pb_t	Isotope ratios					Rho	Age, Ma		
				$^{206}Pb/^{204}Pb^a$	$^{207}Pb/^{206}Pb^b$	$^{208}Pb/^{206}Pb^b$	$^{207}Pb/^{235}U$	$^{206}Pb/^{238}U$		$^{207}Pb/^{235}U$	$^{206}Pb/^{238}U$	$^{207}Pb/^{206}Pb$
1	50–60, one grain, brown, platy	2.87	0.01	3543	0.1214 ± 1	0.0191 ± 1	5.9349 ± 237	0.3545 ± 10	0.67	1966 ± 8	1956 ± 6	1977 ± 5
2	30–40, ten grains, dark brown, pseudoprismatic	2.57	0.09	333	0.1215 ± 2	0.0333 ± 1	5.9571 ± 196	0.3555 ± 10	0.78	1970 ± 6	1961 ± 6	1979 ± 4
3	30–40, eight grains, brown, platy	2.81	0.01	4080	0.1217 ± 1	0.0310 ± 1	6.0529 ± 121	0.3607 ± 7	0.92	1984 ± 4	1986 ± 4	1981 ± 1

* No baddeleyite charge was determined; Pb_c, common lead; Pb_t, total lead; [a]measured isotope ratios; [b]isotope ratios corrected for blank and common lead; Rho, correlation coefficient of error of $^{207}Pb/^{235}U$–$^{206}Pb/^{238}U$ ratios. The error values (2σ) correspond to the last significant digits.

Table 8. Sm–Nd and Rb–Sr isotopic data for dike rocks of the Kola–Murmansk block

Sample	Rock	Sm, μg/g	Nd, μg/g	$^{147}Sm/^{144}Nd$	$^{143}Nd/^{144}Nd$	Error (2σ)	$\varepsilon_{Nd}(T)$
Gabbronorite, Murmansk area, T = 1983 ± 5 Ma							
Sa-539-1	Small-grained dolerite, marginal part of the dike	2.15	9.54	0.13655	0.511895	0.000004	0.72
Sa-539-5	Gabbropegmatite schlieren, dike center	4.29	18.7	0.13835	0.511991	0.000007	2.10
Sample	Rock	Rb, μg/g	Sr, μg/g	$^{87}Rb/^{86}Sr$	$^{87}Sr/^{86}Sr$	Error (2σ)	$(^{87}Sr/^{86}Sr)_T$
Gabbronorite, Murmansk area, T = 1983 ± 5 Ma							
Sa-539-1	Small-grained dolerite, marginal part of the dike	17.7	221	0.2316	0.708615	0.000010	0.701739
Sa-539-5	Gabbropegmatite schlieren, dike center	12.9	189	0.1982	0.708571	0.000011	0.702688

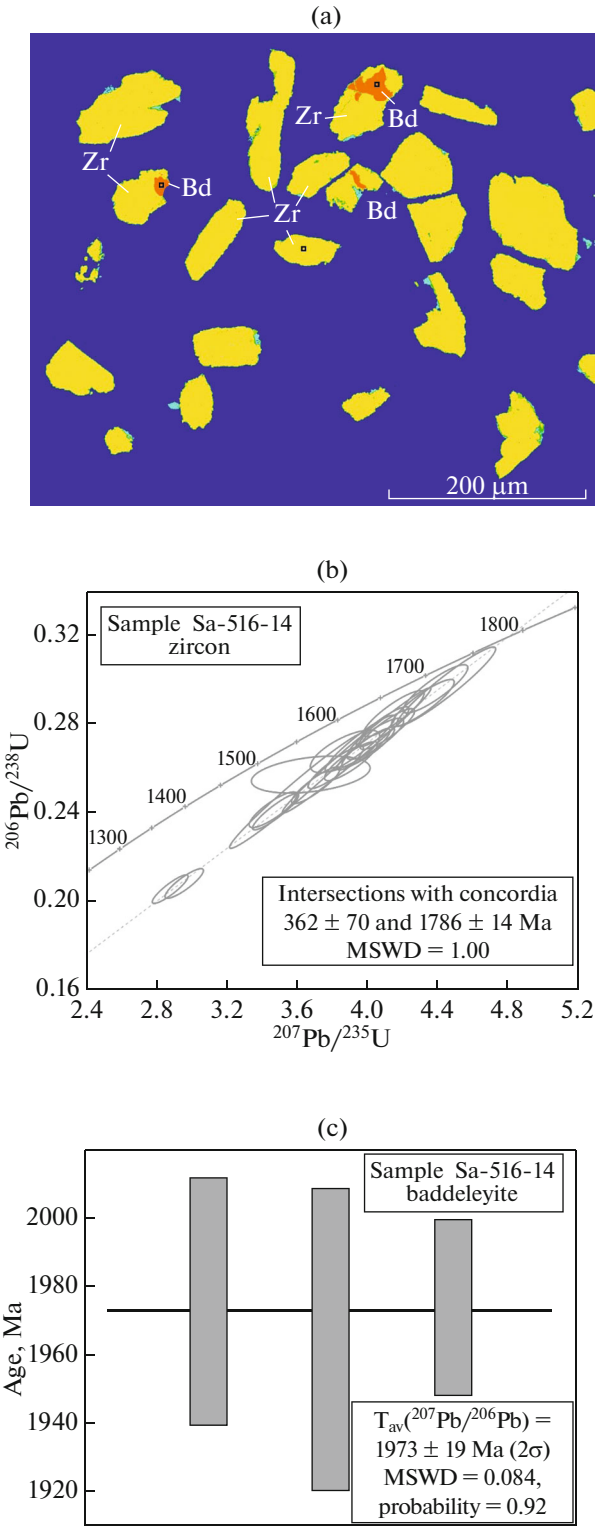

Fig. 11. (a) Contrasting cathodoluminescent image of zircons from metamorphosed ferropicrite (Sample Sa-516-14); (b) plot with concordia for zircons; (c) estimate of weighted average $^{207}Pb/^{206}Pb$ age of baddeleyite from metamorphosed ferropicrite (Sample Sa-516-14). Zr, zircon; Bd, baddeleyite. Black squares show the areas of microprobe analysis.

for gabbronorite from a dike in the Murmansk area, as well as in dikes of the Nyasukka swarm of the northern frame of the Pechenga structure (Smolkin et al., 2015).

Geochemistry of Dikes and Sills

The metadolerites of dikes of the Kirkenes area have low Fe_2O_{3total} and TiO_2 contents and moderate alkalinity corresponding to the average compositions of basaltic rocks of the above-described volcano-sedimentary formations (Fig. 12, Table 9). The rocks contain relatively low contents of Ni, Cr, V, and Cu, similar to the Kolasjoki volcanic rocks. At the same time, we should note the absence of Zr minimum in metadolerites and the presence of negative Nb anomaly (Nb/Nb* ~ 0.6) (Fig. 13a) in contrast to the Kolasjoki and Kuetsjarvi volcanic rocks. In the pattern of trace elements ($(La/Sm)_N$ = 1.6–2.2, $(Gd/Yb)_N$ = 1.2–1.7), they correspond to E-MORBs.

The gabbronorites from large dikes exhibit in situ differentiation with mafic cumulates at the bottom and accumulation of incompatible elements in the upper part of the body as schlieren aggregates (Fig. 13c, Table 9). The absence of noticeable anomalies of most trace elements (excluding Sr), the REE pattern ($(La/Sm)_N$ = 2.2–2.4, $(Gd/Yb)_N$ = 1.3–1.4), and the absence of Eu anomaly (Eu/Eu* = 0.94–1.06) allow us to ascribe them to E-MORBs.

Ferropicrites of dikes of the Murmansk and Kola–Norwegian terranes have high Fe_2O_{3total} and TiO_2 contents (up to 21 and 4.5 wt %, respectively), meaning that they can be considered as subvolcanic analogs of the Pilgujarvi rocks of the Pechenga structure. At the same time, the comparative analysis of most Mg members of ferropicrite series shows significant enrichment of ferropicrites of dikes in alkalis along with relatively lower CaO contents. All ferropicrites are characterized by high Ni, Co, and Cr contents; the positive correlation of Ni and Cr with MgO indicates the olivine and titanomagnetite control of their crystallization. Significantly uneven variations in LILE contents are mostly typical of rocks of quenching zones of all dike types, which is most likely related to metamorphic alteration. The maximum U and Th contents in picrites which are located in Ura Guba area (Fig. 13c) are probably caused by U–Th mineralization found in pegmatoids and related metasomatites (Kaulina et al., 2017).

Similarity of ferropicrites from dikes of different regions is responsible for negative Sr anomaly (Sr/Sr* ~ 0.4) in combination with Ti maximum and minor Zr minimum (Zr/Zr* ~0.8), which is most typical of differentiated bodies of the Nyasukka swarm (Fig. 13b). The presence of the clearly expressed negative Sr anomaly is probably a primary geochemical feature of ferropicrites and gabbronorites and characterizes the initial mafic melts. The Sr anomaly (Sr/Sr*) is positively correlated with the bulk CaO content of rocks.

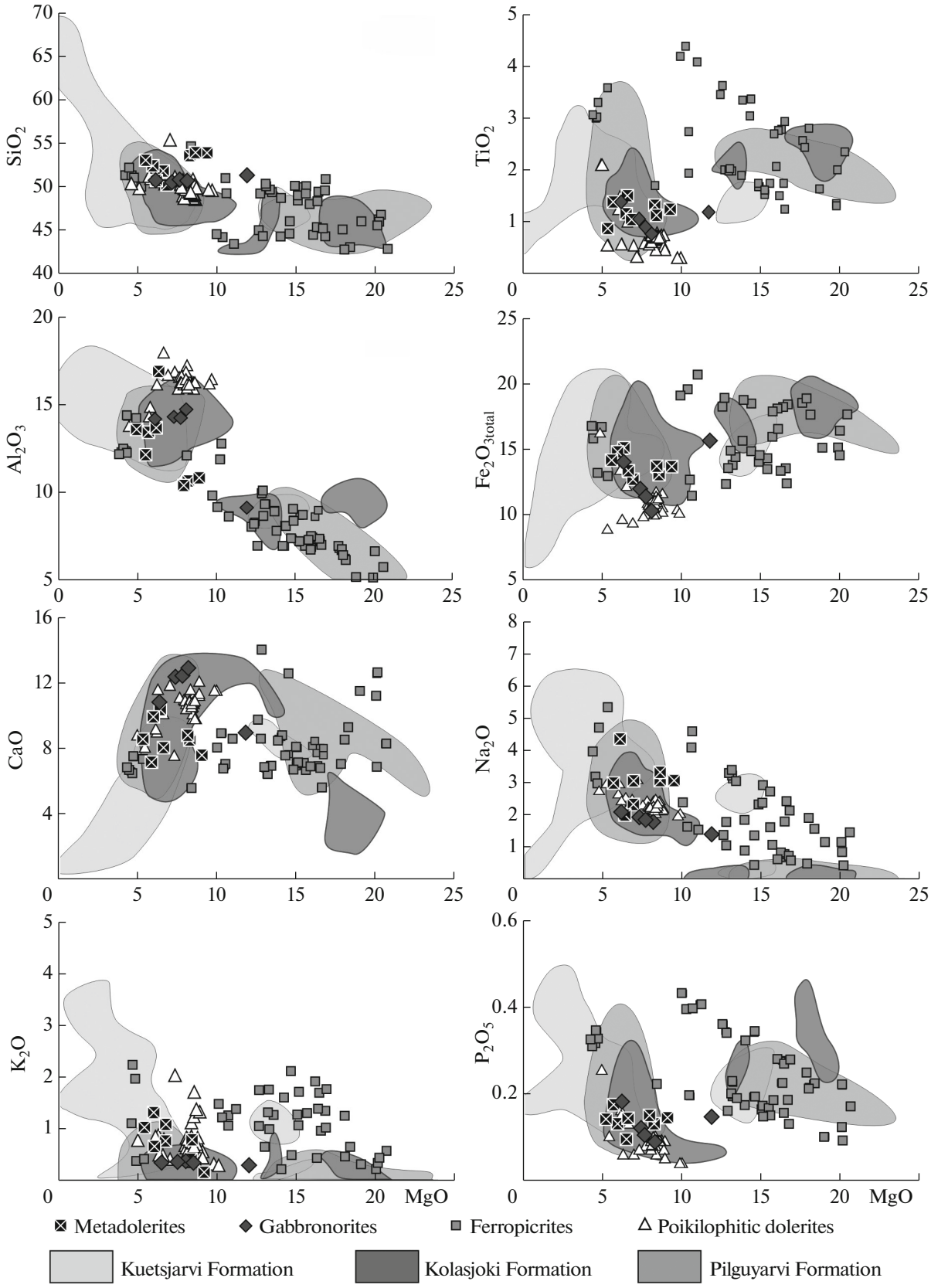

Fig. 12. MgO–oxide plot (wt %) for the Early Proterozoic dikes of the Kola–Murmansk region. Fields show the composition of rocks of the Kuetsjarvi, Kolasjoki, and Pilguyarvi formations of the Pechenga structure.

Table 9. Contents of major oxides (wt %) and trace elements (ppm) of representative samples of dikes of gabbronorites (GbN), ferrodolerites (FeDlr), and ferropicrites (FePic)

Rock	FePic	FePic	FePic	FePic	FePic	GbN	FeDlr	FeDlr[1]
Area	Liin	Nyas	Ura	Sneg	Olen	Murm	Olen	Olen
Sample	516-1	596-1	598-1	536-1	613-3	539-3	626-1	626-2
SiO_2	43.82	44.87	44.75	43.30	41.49	50.11	49.85	49.10
TiO_2	2.68	1.30	1.90	2.22	2.33	1.00	2.27	2.61
Al_2O_3	7.04	4.97	6.39	7.39	6.39	14.00	12.95	12.79
$Fe_2O_{3\ total}$	17.66	14.70	15.76	16.66	18.07	11.73	16.18	17.78
MnO	0.21	0.20	0.21	0.19	0.22	0.19	0.21	0.22
MgO	16.12	19.83	19.40	16.36	17.50	7.47	5.15	4.44
CaO	7.81	10.98	6.58	8.19	8.26	12.20	9.23	8.73
Na_2O	0.62	1.07	0.41	1.04	1.74	1.92	2.70	2.78
K_2O	0.94	0.33	0.41	1.07	0.47	0.41	0.78	0.92
P_2O_5	0.27	0.12	0.21	0.23	0.21	0.13	0.21	0.24
S_{total}	0.08	0.22	0.09	0.05	0.16	0.09	0.08	0.10
LOI	2.21	0.73	3.32	2.74	2.57	0.49	0.10	0.00
Total	99.46	99.32	99.43	99.44	99.41	99.74	99.71	99.71
Li	17.3	6.50	17.5	20.4	5.50	8.37	6.52	6.80
Sc	29.6	42.3	22.9	22.8	29.1	37.8	36.5	33.9
V	299	248	221	256	247	251	376	361
Cr	966	1663	1236	1002	1143	305	94.8	54.9
Co	98.8	104	90.2	82.9	97.9	43.0	48.5	48.2
Ni	888	784	911	812	824	93.7	81.6	65.3
Cu	136	684	122	139	194	106	285	327
Zn	181	88.1	133	113	119	78.1	141	155
Ga	13.5	9.21	11.9	11.0	13.2	12.0	19.6	21.2
Rb	28.8	8.87	11.7	41.0	12.8	13.8	22.6	26.6
Sr	68.5	149	77.8	123	287	139	201	208
Y	18.6	11.7	14.0	13.3	13.9	16.2	30.4	33.7
Zr	109	56.9	108	126	114	65.2	142	178
Nb	21.3	8.31	19.8	16.5	18.8	11.6	13.1	15.2
Mo	1.01	1.22	0.61	0.67	1.04	0.81	1.18	1.61
Cs	1.01	0.22	2.77	2.70	0.38	0.40	0.59	0.65
Ba	178	90.1	76.6	202	157	134	203	236
La	19.1	8.80	16.5	15.4	16.2	11.2	17.8	21.6
Ce	40.4	21.0	37.4	33.5	40.0	21.9	42.0	49.5
Pr	5.93	3.05	5.16	4.85	5.09	3.07	5.54	6.48
Nd	28.3	13.1	21.1	22.0	22.5	13.7	23.9	27.9
Sm	6.44	3.49	4.89	4.34	5.37	3.12	6.00	7.10
Eu	2.23	1.06	1.49	1.59	1.85	1.00	1.86	2.05
Gd	6.31	3.43	4.67	4.86	5.14	3.38	6.46	7.33
Tb	0.86	0.53	0.66	0.66	0.70	0.61	1.00	1.14
Dy	4.89	2.68	3.37	3.57	3.85	3.48	6.20	7.03
Ho	0.78	0.54	0.62	0.63	0.63	0.72	1.23	1.41
Er	1.93	1.27	1.48	1.63	1.65	2.22	3.51	3.95
Tm	0.26	0.17	0.19	0.20	0.22	0.32	0.52	0.58
Yb	1.53	1.03	1.20	1.24	1.28	2.03	3.24	3.66
Lu	0.19	0.15	0.17	0.16	0.17	0.30	0.47	0.52
Hf	3.05	1.78	2.87	3.24	3.23	1.88	3.79	4.24
Ta	2.37	0.79	1.30	1.10	1.20	0.69	0.81	0.92
Pb	2.51	3.11	1.71	1.93	2.04	2.97	4.20	4.89
Th	1.71	0.83	2.32	1.53	1.81	1.64	3.09	3.70
U	0.54	0.19	0.63	0.45	0.42	0.42	0.67	0.86

Dike areas: Liin, settlement of Liinahamari; Nyas, Nyasukka; Ura, Ura Guba; Sneg, town of Shezhnogorsk; Olen, town of Olenegorsk; Murm, city of Murmansk. [1]A schlieren in ferrodolerite dike.

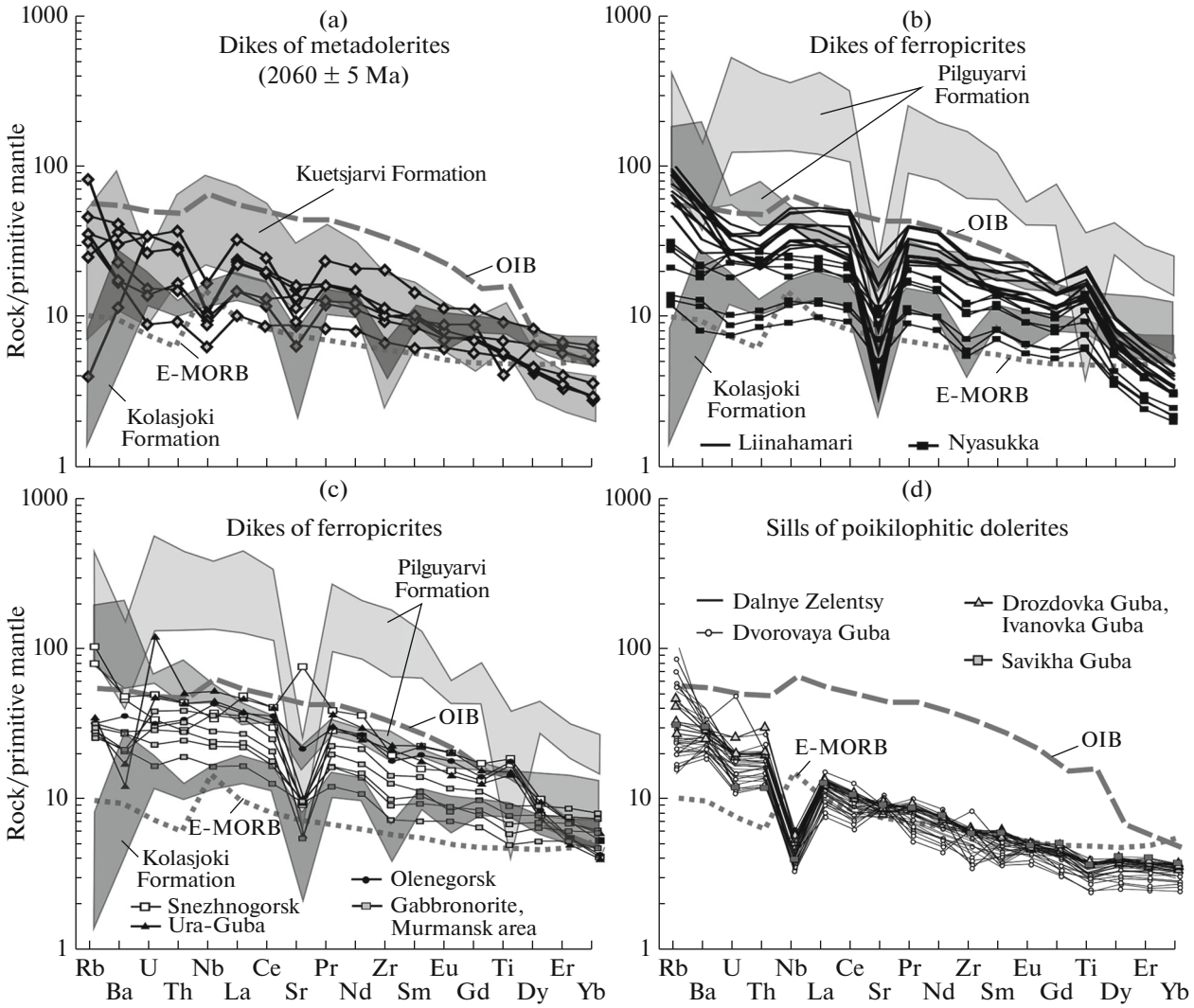

Fig. 13. Contents of trace elements in dikes of the Kola–Murmansk region normalized to primitive mantle. Fields show the composition of rocks of the Kuetsjarvi, Kolasjoki, and Pilguyarvi formations of the Pechenga structure.

The poikilophitic dolerites, which could be considered as the age analogs of the above-described rocks of the southern part of the Pechenga structure and Panarechka caldera, have higher Al_2O_3 and low Fe_2O_3 and TiO_2 contents (Fig. 12). In spite of a relatively large thickness of sills of poikilophitic dolerites, they are weakly differentiated with minor variations in contents of most major oxides. In contents of major oxides, the poikilophite dolerites are similar to rocks of the Kaplya Formation of the Pechenga structure; however, their geochemical features are strongly distinct from those of all volcanic rocks described above. These include negative Nb anomaly (Nb/Nb* = 0.22–0.46) (Fig. 10d), lower REE contents, relatively high $(La/Sm)_N$ ratios (2.0–3.2), low $(Gd/Yb)_N$ values (1.1–1.6), and no Eu anomaly (Eu/Eu* = 0.89–0.97). These rocks are geochemically homogeneous: the REE, HSFE, and LILE contents vary insignificantly, indicating minimum influence of late metamorphic processes.

DISCUSSION

Correlation of Volcanic Series of the Pechenga and Imandra–Varzuga Structures and Dike Complexes

Recent comprehensive studies of the Early Proterozoic sedimentary and volcanic rocks of the northern part of the Pechenga structure (Hanski et al., 2014; Melezhik et al., 2012) allow their correlation with volcano-sedimentary complexes of the Imandra–Varzuga structure and dikes around these structures. The remote position of the Pechenga and Imandra–Varzuga fragments of the entire PPIV belt, complex tectonic setting of the junction zone of volcano-sedimentary sequences, and limited geochronological data indicate an ambiguous geological setting of the formations and complicate the correlation of rocks of the southern and northern parts of the Pechenga structure and, mostly, the correlation of rocks of the latter with rocks of the Imandra–Varzuga structure. On the basis

of geochronological and precise geochemical data, we compared the volcanic rocks of these structures.

As shown by (Hanski et al., 2014), the most important boundary defining the transition from continental to oceanic settings was registered in the change in type of volcano-sedimentary rocks from the Kuetsjarvi Formation to the Kolasjoki Formation. The U–Pb age of zircon from volcaniclastic conglomerates of the upper part of the section of the Kuetsjarvi Formation (2058 ± 2 Ma) was interpreted as the lower age boundary of the Kolasjoki volcano-sedimentary formation (Melezhik et al., 2007). These data are in agreement with the U–Pb age of zircon from a rhyodacite sill at the contact of rocks of the Kuetsjairvi and Kolasjoki formations (2043 ± 18 Ma; Mitrofanov et al., 2001), the U–Pb age of baddeleyite from metadolerite dikes of the Kirkenes area (2060 ± 5 Ma), and the age of similar rocks of adjacent regions (Melezhik et al., 2012).

It can be suggested that subaerial sedimentation and geochemical features of magmatism identified in the Kuetsjarvi rocks of the Pechenga structure are also traced in the Imandra–Varzuga structure, the Umba Formation of which is considered as the age analog of the Kuetsjarvi Formation (Fig. 2). In contrast, the basalts of both the Umba Formation and the overlying Ilmozero Formation are enriched in incompatible elements and have a clear Nb minimum (Fig. 8a) and higher partition coefficients of LREEs ($(La/Sm)_N$ = 2.5–3.1), making them similar to older rocks of the Polisar Formation.

The Kirkenes metadolerite dikes also with weak REE fractionation and positive $\varepsilon_{Nd}(T)$ values can be considered as the subvolcanic analogs of the Kolasjoki tholeiitic basaltic series, the preliminary age of which is 2018 ± 54 Ma (Table 1). However, the presence of negative Nb anomaly (Nb/Nb* ~ 0.6) in metadolerites can be a result of a various degree of their contamination by crustal material.

The volcanic rocks forming the above-lying part of the section of the Imandra–Varzuga structure include the Tominga ferrobasalts and ferropicrites, which are considered as the analog of the Pilguyarvi volcanic rocks (Smolkin, 1997). The comparison of their compositions shows that the Tominga tholeiitic rocks with weak LREE and HREE fractionation are more similar to older Kolasjoki basalts. The geochemical similarity of the latter rocks with Mennel basalts of the southern zone of the Pechenga structure indicates their formation from compositionally similar parental melt as a result of a common magmatic cycle.

The dike magmatism synchronous with origination of E-MORB-type melts beyond the Pechenga structure includes two series, as in the Pilguyarvi Formation. The gabbronorites of the Murmansk area are geochemically identical to the Pilguyarvi ferrobasalts. The age of gabbronorite of 1981 ± 3 Ma indicates synchronous tholeiitic and ferropicritic magmatism in the Pechenga structure. Abundant rocks of ferrobasalt series are identified in the southeastern frame of the Imandra–Varzuga structure. The age of the Ondomozero intrusion (1974 ± 3 Ma) corresponds to the main stage of magmatic activity of the Pechenga structure and the age of gabbronorites indicated above (Galimzyanova et al., 2006). The Pyalochnozero intrusion (1936 ± 9 Ma) and ultramafic intrusions of the Ust-Pyalka River formed synchronously with dikes of the Nyasukka swarm of the northern frame of the Pechenga structure, the age of which is estimated at 1941 ± 3 Ma (Smolkin et al., 2015).

The ferropicrites of dikes abundant in the frame of the Pechenga structure are typically considered as the direct analogs of the ferropicrite series (Borisova, 1989; Smolkin et al., 2015). At the same time, the analysis of the composition shows that subvolcanic ferropicrites (including differentiated bodies of the Nyasyukk swarm), which formed after the main phase of ferropicrite magmatism, have higher (relative to volcanic rocks) alkali contents and different HFSE ratio and REE pattern (Fig. 10). In addition, the Kolasjoki and Pilguyarvi volcanic rocks which filled the axial zones of the structure exhibit features of various various degree of crustal contamination: widely variable Nb/Nb* ratio and $\varepsilon_{Nd}(T)$ value of –2.7 to +3.3 (Hanski, 1992; Skuf'in and Theart, 2005). In contrast, the ferropicrites of dikes are less contaminated ($\varepsilon_{Nd}(T)$ = +1.4 to +3.2). In a consecutive range of derivatives of ultramafic melts with age of 1.98 Ga, the dike magmatism geochemically corresponds to the greatest degree to the rocks of the upper parts of the section of the Pilguyarvi Formation.

The correlation of the Kalevian volcanic rocks is difficult because of almost synchronous activity of various volcanic centers, which produced rocks of contrasting chemical composition. In a series of geochemical features (Nb/Nb*, Sr/Sr*, $(La/Sm)_N$, $(Gd/Yb)_N$), the most primitive ultramafic rocks of the Mennel and Kaplya bimodal volcanic series can be compared with mafic rocks and their derivates of the Pechenga caldera of the Imandra–Varzuga structure. The poikilophitic dolerites which compose the sills in the Murmansk Terrane and could be considered as the subvolcanic analogs of the final stage of the evolution of the belt are geochemically distinct from the above-described Proterozoic subvolcanic rocks. Similar features are typical of almost coeval volcanic rocks of the Por'itash volcanic center of the southern part of the Pechenga structure, as well as the coeval Saminga Formation with the latest rocks in the Panarechka caldera. In spite of some geochemical distinctions, the high Al value, low Ti and Fe contents, and, most important, evident Nb anomaly are the common features of all rocks (Figs. 6f, 8c, 10d).

Thus, the correlation of volcanic rocks of the Pechenga and Imandra–Varzuga structures reveals asynchronous variations in volcanism during regular

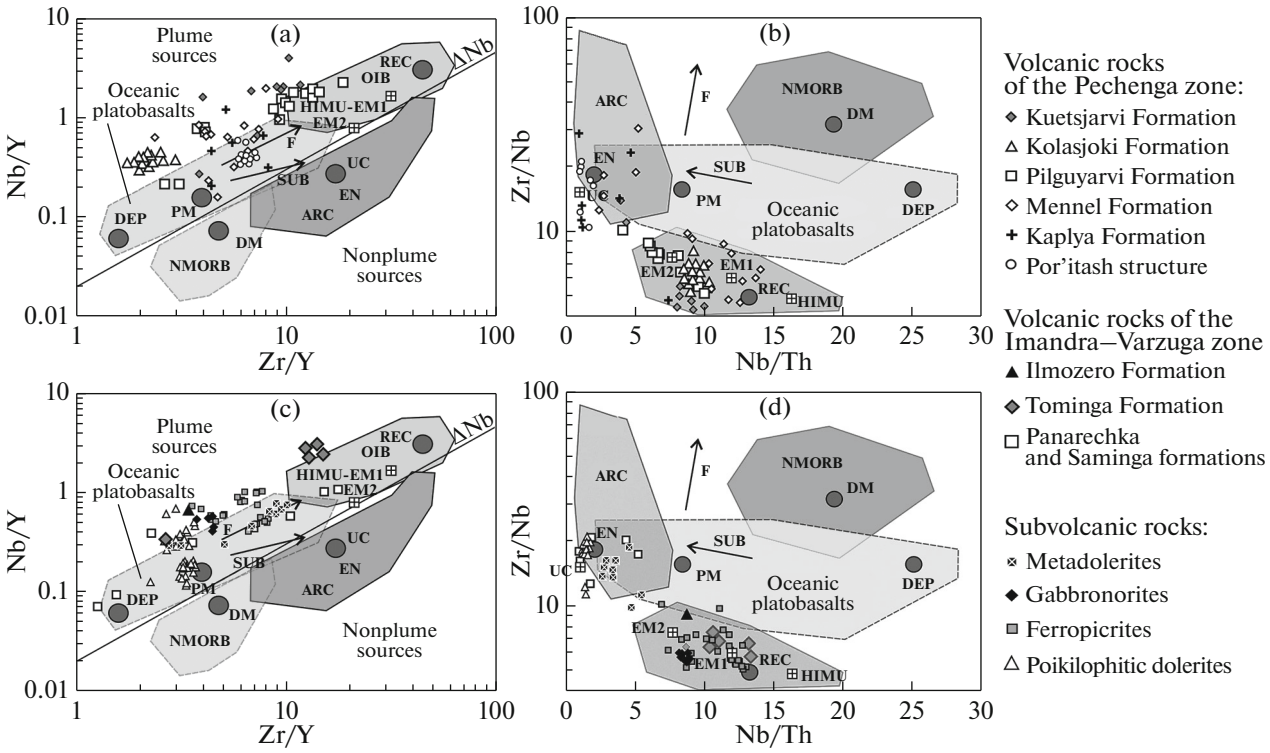

Fig. 14. Zr/Y–Nb/Y and Nb/Th–Zr/Nb plots after (Condie, 2005) for volcanic rocks of the Pechenga zone (a, b), Imandra–Varzuga zone and subvolcanic rocks (c, d). Arrows indicate variation trends of melt compositions during equilibrium melting (F) and as a result of subduction (SUB); UC, continental crust; PM, primitive mantle; DM, upper zone of depleted mantle; HIMU, component of recycled oceanic crust after (Van Keken et al., 2002); EM1 and EM2, enriched mantle sources; ARC, oceanic arc basalts; N-MORB, normal mid-oceanic ridge basalts; OIB, oceanic island basalts; DEP, lower zone of depleted mantle; EN, enriched component; REC, recycling products.

change of geodynamic settings in the range of 2.06–1.86 Ga. In the Pechenga structure, the transition from continental to oceanic settings is recorded by E-MORB series in the structure of the Kolasjoki Formation at 2058–2018 Ma (Hanski et al., 2014). In contrast, the volcanic rocks of this age of the Imandra–Varzuga structure retain geochemical features of continental settings. The geodynamic setting in the eastern part of the belt probably changed later and resulted in intrusion of mostly ferrobasaltic melts (the Tominga volcanic rocks) and intrusions of the Ondomozero group in the southeastern frame of the structure.

Sources and Evolution of Proterozoic Magmatism of the Polmak–Pechenga–Imandra–Varzuga Belt at 2.06–1.86 Ga

In spite of available isotopic-geochemical evidence of the involvement of plume-lithospheric interaction processes in the formation of the PPIV Belt (Walker et al., 1997), the problem of their scales and conditions of formation of strongly contrasting melts for more than 200 m.y. is a matter of debate (Hanski, 1992; Melezhik et al., 2012; Smolkin, 1992, 1997). Recent isotopic and geochemical data significantly refine the geodynamic settings and evolutionary stages of the Pechenga and Imandra–Varzuga structures outlined by Smolkin (1997). The Zr/Y–Nb/Y ratios are geochemical indicators which discriminate between plume and shallower (e.g., the level of origination of N-MORBs) magmatism (Figs. 14a, 14c). The data points of compositions of all volcanic rocks and dike series occur within plume sources above the discriminant line ΔNb. The Nb/Th–Zr/Nb plot (Figs. 14b, 14d) shows that enriched lithospheric mantle which produced melts with low Zr/Nb ratios was a possible source for primary melts of the Kuetsjarvi, Kolasjoki, and Pilguyarvi series and their homologs of the Imandra–Varzuga structures.

The geochemical data, as well as the isotopic features of rocks, were the basis for identification of autonomous tholeiitic and ferropicritic igneous series in the structure of the Pilguyarvi Formation, which occur in both the northern and southern parts of the Pechenga structure (Hanski and Smolkin, 1995; Skuf'in and Theart, 2005; Smolkin, 1992). The geochemical features of tholeiitic rocks definitely indicate their primary mantle origin with minor impact of crustal-mantle interaction. The most primitive melts which best correspond to the features of tholeiitic E-MORBs and OIBs include the Kolasjoki and Pilguyarvi basalts of the

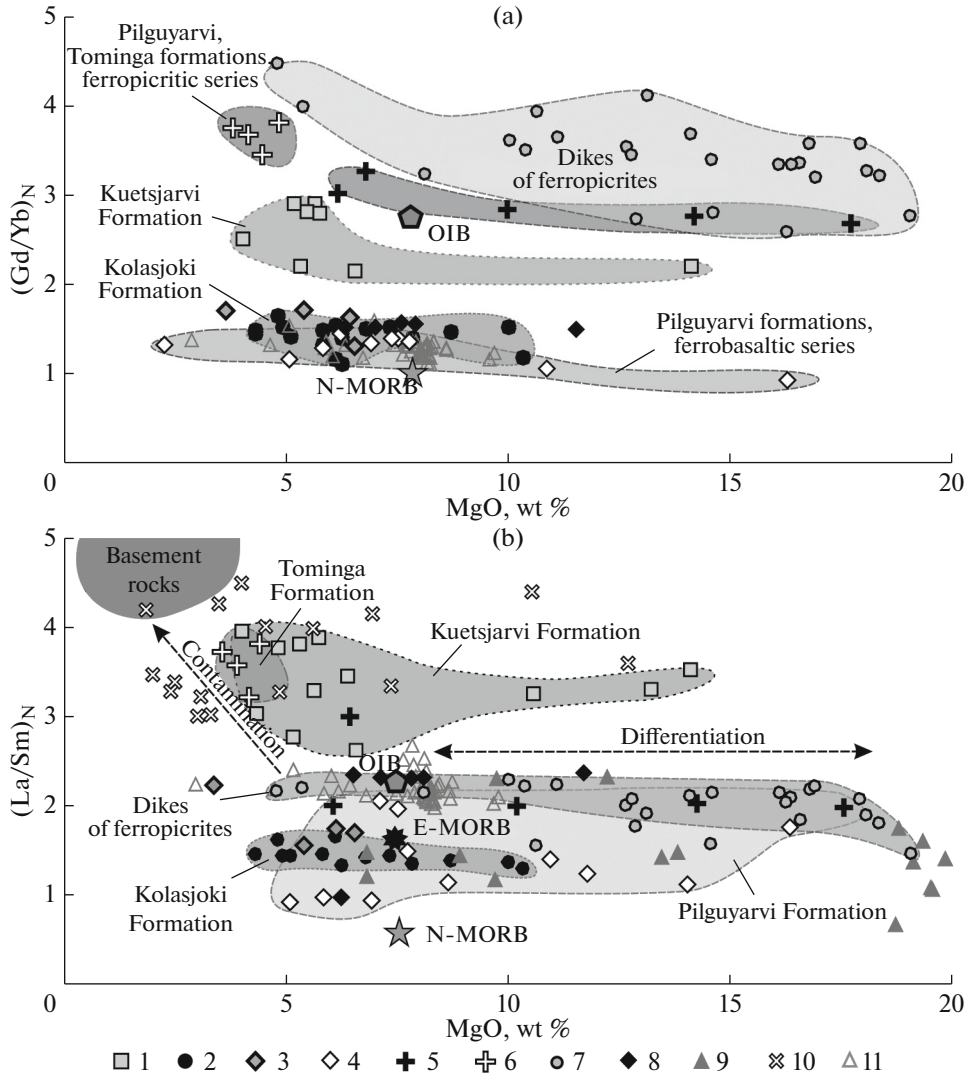

Fig. 15. (a) MgO–$(Gd/Yb)_N$ and (b) MgO–$(La/Sm)_N$ plots for volcanic rocks, dikes, and sills with age of 2.06–1.86 Ga. (1) Kuetsjarvi Formation; (2) Kolasjoki Formation; (3) metadolerite dikes with age of 2.06 Ga; (4, 5) Pilguyarvi Formation: (4) ferrobasalts, (5) ferropicrites; (6) Tominga Formation; (7, 8) frame dikes: (7) ferropicrites, (8) gabbronorites; (9) Mennel Formation; (10) Kaplya Formation; (11) poikilophitic dolerites. The N-MORB, E-MORB, and OIB values are given after (McDonough and Sun, 1995).

Pechenga structure with typical low $(La/Yb)_N$ values. The ferropicritic melts were generated from an autonomous source related to activation of a metasomatized mantle reservoir beyond the garnet stability levels (Hanski and Smolkin, 1995).

On the MgO–$(Gd/Yb)_N$ plot (Fig. 15), the data points of compositions of the Kuetsjarvi and Kolasjoki volcanic rocks, as well as Pilguyarvi ferrobasalts, form a trend with a regularly decreasing $(Gd/Yb)_N$ ratio. It is almost unaffected by crustal contamination, but reflects the involvement of garnet in the generation area of mantle melts. Thus, this trend is caused by regular uplift of the magma generation zone from the garnet stability level (Kuetsjarvi Formation) to shallower mantle facies of spinel lherzolites (the Pilguyarvi ferrobasalts). In geodynamic respect, the evolution of plume-lithospheric process, which led to the change in geochemical features of primary melts and the depth of formation of sublithospheric mantles, was responsible for the decreasing thickness of continental lithosphere in the axial part of the PPIV belt.

Within this model, however, we should take into account the involvement of ferropicrite melts, which formed at late stages of the evolution of the belt within the Pechenga and Imandra–Varzuga structures and also filled numerous fault zones of the Archean basement in its frame (ferropicrite dikes). Judging from the fractionated HREE patterns, the formation of these rocks was probably related to the deeper mantle source at the level of garnet lherzolite facies. The enrichment

of ferropicrites in incompatible elements combined with high positive $\varepsilon_{Nd}(T)$ values indicates the involvement of the metasomatized mantle component in the generation zone of ferropicrite melts (Smolkin, 1997). The isotopic features of rocks point to fertilization of mantle substrate directly prior the intrusion of ferropicrite melts. The final stage of magmatism of the belt, which mostly produced the volcanic rocks of the southern part of the Pechenga structure and Panarechka caldera, indicates the generation of melts from both the level of facies of spinel lherzolites and the level of facies of garnet lherzolites.

The estimation of the role of mantle sources is directly related to the geodynamic settings of the formation of volcanic sequences of the PPIV belt. The Kuetsjarvi volcanic rocks of the Pechenga structure and their analogs in the Imandra–Varzuga structure exhibit geochemical features of a deep mantle source with a minor contribution of crustal contamination, e.g., the high $(Gd/Yb)_N$ and $Nb/Nb^* \geq 1$ and low Zr/Nb ratios. These rocks have also a low-radiogenic isotopic Nd composition ($\varepsilon_{Nd}(T) < 0$), indicating the involvement of a source which was enriched in incoherent elements ($(Nd/Sm)_N >$ CHUR) long before the formation of melts. The model age ($T_{Nd}(DM)$) of the Kuetsjarvi volcanic rocks of 2.51–2.87 Ga calculated from data of (Hanski et al., 2014; Skuf'in and Theart, 2005; Skuf'in and Bayanova, 2006) indicates the Neoarchean age of separation of the melt protolith from depleted mantle and shows that this source could have been related to asthenospheric or lithospheric mantle metasomatically reworked in the Archean. In contrast, the positive ε_{Nd} value of +1.7 and the low primary $(^{87}Sr/^{86}Sr)_i$ ratio of 0.70166 of metadolerite dike of the Kirkenes area and dikes of the Nyasukka swarm of the northern frame of the Pechenga structure (Smolkin et al., 2015) mostly reflect primary magmas of volcanic series of this period and indicate the asthenospheric nature of the melt source. Thus, the mafic volcanism of the axial part of the Pechenga structure in the range of 2.06–1.98 Ga demonstrates the regular change in Nd isotopic characteristics related to the decreasing role of the lithospheric source, whereas the dikes which filled the fault zones of the Archean basement in the frame of the structure retained the primary Nd isotopic characteristics of mafic melt. The minor involvement of an enriched reservoir in melts of the distal zone of the Pechenga structure is evident from Rb–Sr isotopic features of metadolerite and gabbronorite dikes. The isotopic $Sr_i(T)$ ratio calculated for 2060 and 1980 Ma, respectively, exhibits no significant isotopic shift due to the contribution of the radiogenic component (Fig. 7), which can also indicate a short tectonomagmatic pulse resulting in the formation of feather faults filled with mafic melt in the northern frame of the Pechenga structure.

Recent isotopic-geochronological studies show that magmatism with features of intracontinental tholeiites changed at 2.06–2.02 Ga (Hanski et al., 2014). The age boundary of 2.06 Ga, which reflects the change of geodynamic setting, was registered also in the Lomagundian–Jatulian anomaly of heavy C isotope ($\delta^{13}C$), which is typical of significant territory of the Fennoscandian Shield (Lahtinen et al., 2005; Wanke and Melezhik, 2005). The estimates by Daly et al. (2006), which, however, are interpreted as the age of opening of adjacent Laplandia–Kola Ocean rather than the Pechenga–Varzuga one, coincide with the age of ~2.05 Ga. The change in redox conditions evident from a variable Fe# value ($Fe^{3+}/(Fe^{3+} + Fe^{2+})$) of the Kuetsjarvi rocks is an important marker of the end of subaerial volcanism (Hanski et al., 2014). Our calculation of this ratio for representative sampling of volcanic rocks of the Pechenga structure ($n = 390$) shows that the average Fe# value of the Kuetsjarvi rocks is 0.54 ± 0.31 in contrast to 0.22 ± 0.28 (more oxidized Fe) of later Kolasjoki and Pilguyarvi rocks. The comparison of these values with data on volcanic rocks of the Imandra–Varzuga structure ($n = 116$) shows that iron in the Umba volcanic rocks is more oxidized (Fe# = 0.47 ± 0.18) relative to the Kuetsjarvi rocks, which can reflect the variable conditions of volcanic activity. At the same time, the Ilmozero and Tominga rocks have Fe# values similar to those of analogous rocks of the Pechenga Group (0.25 ± 0.21 and 0.23 ± 0.18, respectively).

The comparison of geochemical and isotopic data on the Pilguyarvi and Tominga volcanic rocks indicates that they belong to two series with minor crustal component, the formation of which was affected by the asthenospheric source. The first series, which best corresponds to E-MORB-type tholeiites, includes the Pilguyarvi and Kolasjoki ferrobasalts of the Pechenga structure and gabbronorites of dikes from the Murmansk area and Tominga Formation of the Imandra–Varzuga structure with typical lowest $(La/Yb)_N$ values (Fig. 15b). The second series includes the Pilguyarvi ferropicrites, comagmatic gabbrowehrlite intrusion, and dike series with positive $\varepsilon_{Nd}(T)$ values and higher $(La/Yb)_N$ ratio, indicating the asthenospheric nature of melts.

The evolution of magmatism of the Pechenga and, to a lesser degree, Imandra–Varzuga structures is considered in detail in (Hanski, 1992; Sharkov and Smolkin, 1997; Smolkin, 1992, 1997) and, taking into account the recent data on the genesis of sedimentary rocks, by Melezhik et al. (2012). On the basis of data on the Pechenga structure, the age boundary of transition from continental to oceanic conditions and the corresponding change in magmatism were identified (Hanski et al., 2014). The Kuetsjarvi volcanic rocks contaminated with crustal material were replaced by Kolasjoki and further Pilguyarvi rocks geochemically similar to E-MORBs. Further evolution is traced in the southern part of the Pechenga structure, where mafic melts and their differentiates form a reverse

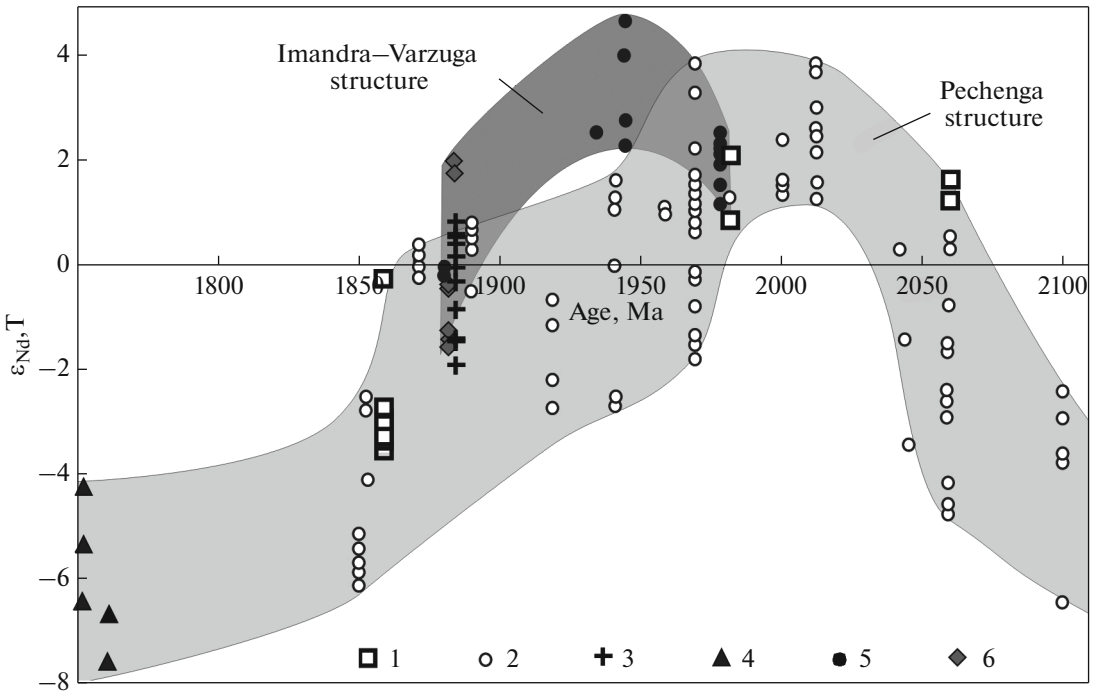

Fig. 16. Plot of $\varepsilon_{Nd}(T)$ variation in Proterozoic igneous rocks of the northeastern part of the Fennoscandian Shield in the interval of 2.10–1.75 Ga. (1) Dike complexes; (2) volcanic rocks of the Pechenga zone; (3) mafic rocks of Gremyakha–Vyrmes block; (4) granitoids of the Litsa–Araguba complex; (5) volcanic rocks and mafic intrusions of the Imandra–Varzuga zone; (6) rocks of Soustov pluton. The data on dike complexes (1) are original; the data on other rocks (2–6) are from (Arzamastsev et al., 2006; Bayanova, 2004; Bea et al., 2001; Galimzyanova et al., 2006; Hanski, 1992; Hanski et al., 2014; Skuf'in and Bayanova, 2006; Skuf'in et al., 2013; Smolkin, 1992; Vetrin, 2014).

trend from the most primitive E-MORB melts to andesites, dacites, and rhyolites, which reflect the increasing amount of enriched ancient crustal component. This trend is traced in Sm–Nd isotopic characteristics of rocks and is shown in the $\varepsilon_{Nd}(T)$ vs. time plot (Fig. 16). The most depleted ferropicrite melts with maximum positive $\varepsilon_{Nd}(T)$ values in the Pechenga structure formed at 2060–1970 Ma. Later volcanism is characterized by a gradual decrease in ε_{Nd} to negative values in the latest differentiates of the southern part of the structure.

This evolutionary volcanism of the Pechenga and Imandra–Varzuga fragments of the belt has no support from geochemical features of volcanic rocks in correlated formations of these structures. First of all, as was shown above, the geochemical features of the Tominga Formation, the sedimentary sequences of which are correlated with Pilguyarvi sedimentary rocks, indicate a significant involvement of crustal material in the formation of its volcanic rocks. This is most evident from the MgO–$(La/Sm)_N$ plot (Fig. 15b), where the data points of the Tominga basalts (in contrast to Pechenga analogs) exhibit the most contaminated compositions. The available isotopic-geochronological data on intrusive complexes of the southeastern frame of the Imandra–Varzuga structure (Galimzyanova et al., 2006) allow determination of the period of the formation of mantle melts with maximum $\varepsilon_{Nd}(T)$ values in this structure. Significant distinctions in age identified from the U–Pb age of zircon for the Ondomozero (1974 ± 3 Ma) and Pyalochnozero (1944 ± 14 Ma) ultramafic intrusions (Galimzyanova et al., 2006) show that the peak of the formation of the most isotopically depleted melts in the Imandra–Varzuga structure was shifted relative to the age of the formation of Pechenga analogs by more than 20 m.y. Judging from this, we can suggest asynchronous evolution of volcanism in the Pechenga and Imandra–Varzuga structures.

CONCLUSIONS

The Proterozoic mafic rocks with age of 2.06–1.86 Ga abundant in the Pechenga and Imandra–Varzuga structures and their framing record the main stages of their evolution and reflect the dramatic changes in plume magmatism manifested in composition of volcanic complexes and dike series. The origination of volcanic rocks of the Kuetsjarvi Formation of the Pechenga structure and their analogs in the Imandra–Varzuga structure, judging from geochemical features, is related to a noncontaminated crustal component of a deep mantle source (probably, asthenospheric or lithospheric mantle metasomatically reworked in the Archean). In contrast, the DM source

with separation of the melt above the garnet stability depth was involved in the formation of volcanic rocks of the Kolasjoki Formation and the correlated Ilmozero Formation weakly contaminated with crustal material, as well as the metadolerite dikes of the Kirkenes area. The formation of volcanic rocks of the Pilguyarvi Formation is related, judging from geochemistry, to two mantle sources of various depths, which produced tholeiitic and ferropicritic melts.

The comparative analysis of the volcanic rocks of the Pechenga and Imandra–Varzuga structures shows that their volcanism regularly changed with significant time lapse. The volcanic rocks of the Tominga Formation with continental geochemical features can hardly be correlated with those of Pilguyarvi Formation. The isotopic-geochemical data on igneous rocks of the southeastern part of the Imandra–Varzuga structure indicate later (relative to the Pechenga structure) intrusion of depleted mantle melts, which mostly include tholeiitic series. Thus, the most depleted mantle melts in the Pechenga and Imandra–Varzuga structures were the most active at 2010–1970 and 1970–1890 Ma, respectively.

The analysis of rocks of the Ludicovian cycle of magmatic activity shows the regular change in isotopic-geochemical features, which reflects the gradual uplift of the magma generation zone from the levels of mantle facies of garnet lherzolites with tholeiitic melts of the Kuetsjarvi Formation with age of 2.06–2.04 Ga to the levels of mantle facies of spinel lherzolites with basalts and dolerites of volcanic and dikes series of the Kolasjoki, Tominga, and Pilguyarvi formations at 1.98 Ga. The ongoing activity of the deeper source enriched in incoherent elements at the level of mantle facies of garnet lherzolites led to the formation of the main volume of ferropicritic melts of the Polmak–Pechenga–Imandra–Varzuga Belt and subvolcanic rocks of its framing.

ACKNOWLEDGMENTS

We are grateful to A.B. Vrevskii (Institute of Precambrian Geology and Geochronology, Russian Academy of Sciences) and N.E. Kozlov (Geological Institute, Kola Science Center, Russian Academy of Sciences) for kind and fruitful criticism.

FUNDING

This work was supported by the Russian Science Foundation, project no. 16-17-10260.

Reviewers A.B. Vrevskii, N.E. Kozlov, and A.B. Kotov

REFERENCES

Arzamastsev, A.A., Bea, F., Arzamastseva, L.V., and Montero, P., Proterozoic Gremyakha–Vyrmes Polyphase Massif, Kola Peninsula: An example of mixing basic and alkaline mantle melts, *Petrology*, 2006, vol. 14, no. 4, pp. 361–389.

Arzamastsev, A.A., Fedotov, Zh.A., and Arzamastseva, L.V., *Daikovyi magmatizm severo-vostochnoi chasti Baltiiskogo shchita* (Dike Magmatism in the Northeastern Baltic Shield), St. Petersburg: Nauka, 2009 [in Russian].

Balagansky, V.V., Bogdanova, M.N., and Kozlova, N.E., *Strukturno-metamorficheskaya evolyutsiya severo-zapadnogo Belomor'ya* (Structural–Metamorphic Evolution of the Northwest White Sea Region), Apatity: Izd. Kol'sk. Fil. Akad. Nauk SSSR, 1986 [in Russian].

Balashov, Yu.A., Paleoproterozoic geochronology of the Pechenga–Varzuga structure, Kola Peninsula, *Petrology*, 1996, vol. 4, no. 1, pp. 1–22.

Bayanova, T.B., *Vozrast repernykh geologicheskikh kompleksov Kol'skogo regiona i dlitel'nost' protsessov magmatizma* (Age of the Reference Geological Complexes of the Kola Region and the Duration of Magmatic Processes), St. Petersburg: Nauka, 2004 [in Russian].

Bayanova, T.B., Mitrofanov, F.P., and Egorov, D.G., U-Pb Dating of the Dike Complex at the Kirovogorsk Deposit in the Iron Ore Formation of the Kola Peninsula, *Dokl. Akad. Nauk*, 1998, vol. 360, no. 5, pp. 637–640.

Bea, F., Arzamastsev, A., Montero, P., and Arzamastseva, L., Anomalous alkaline rocks of Soustov, Kola: evidence of mantle-derived metasomatic fluids affecting crustal materials, *Contrib. Mineral. Petrol.*, 2001, vol. 140, pp. 554–566.

Borisova, V.V., A new occurrence of the Nyasyuk-type magmatism in the Kola Peninsula, in *Roi maficheskikh daek kak indikatory endogennogo rezhima* (Mafic Dike Swarms as Indicators of Endogenic Regime), Apatity: Izd. Kol'sk. Fil. Akad. Nauk SSSR, 1989, pp. 17–25.

Condie, K.C., High field strength element ratios in Archean basalts: a window to evolving sources of mantle plumes? *Lithos*, 2005, vol. 79, pp. 491–504.

Daly, J.S., Balagansky, V.V., Timmerman, M.J., and Whitehouse, M.J., The Lapland–Kola orogen: Palaeoproterozoic collision and accretion of the northern Fennoscandian lithosphere, in *European Lithosphere Dynamics, 32nd ed.*, Gee, D.G. and Stephenson, R.A. Eds., *Geol. Soc. London Mem.*, 2006, pp. 579–598.

Fedotov, Zh.A., *Evolyutsiya proterozoiskogo vulkanizma vostochnoi chasti Pechengsko-Varzugskogo poyasa (petrogeokhimicheskii aspekt)* (Evolution of Proterozoic Volcanism in the Eastern Part of the Pechenga–Varzuga Belt (Petrogeochemical Aspect)), Apatity: Izd. Kol'sk. Fil. Akad. Nauk SSSR, 1985 [in Russian].

Fedotov, Zh.A., Bayanova, T.B., and Serov, P.A., Spatiotemporal relationships of dike magmatism in the Kola region, the Fennoscandian Shield, *Geotectonics*, 2012, vol. 46, no. 6, pp. 412–426.

Galimzyanova, R.M., Bayanova, T.B., Neradovskii, Yu.N., and Zhavkov, V.A., The Late Proterozoic mafic intrusions in the eastern part of the Kola Region: new geological and isotope–geochemical data, in *Mater. III Ross. Konf. po izotopnoi geokhronol. "Izotopnoe datirovanie protsessov rudoobrazovaniya, magmatizma, osadkonakopleniya i metamorfizma"* (Proc. 3rd Russ. Isotope Geochronol. Conf. "Isotopic Dating of Ore Genesis, Magmatism, Sedimentation, and Metamorphism"), Moscow, 2006, vol. 1, pp. 183–188.

Hannah, J.L., Stein, H.J., Zimmerman, A., Yang, G., Markey, R.J., and Melezhik, V.A., Precise 2004 ± 9 Ma Re–Os

age for Pechenga black shale: comparison of sulfides and organic material, in *Goldschmidt Conf. Abstracts. Geochim. Cosmochim. Acta, Suppl.*, 2006, vol. 70, A228.

Hanski, E.J., Petrology of the Pechenga ferropicrites and cogenetic, Ni-bearing gabbro-wehrlite intrusions, Kola Peninsula, Russia. Acad. Diss., *Bull. Geol. Surv. Finland*, 1992, vol. 367, pp. 1–192.

Hanski, E.J. and Smolkin, V.F., Pechenga ferropicrites and other early Proterozoic picrites in the eastern part of the Baltic Shield, *Precambrian Res.*, 1989, vol. 45, pp. 63–82.

Hanski, E.J. and Smolkin, V.F., Iron- and LREE-enriched mantle source for early Proterozoic intraplate magmatism as exemplified by the Pechenga ferropicrites, Kola Peninsula, Russia, *Lithos*, 1995, vol. 34, pp. 107–125.

Hanski, E., Huhma, H., Smolkin, V., and Vaasjoki, M., The age of ferropicritic volcanism comagmatic and Ni-bearing intrusions at Pechenga, Kola Peninsula, USSR, *Bull. Geol. Surv. Finland*, 1990, vol. 62, pp. 123–133.

Hanski, E.J., Huhma, H., and Melezhik, V.A., New isotopic and geochemical data from the Palaeoproterozoic Pechenga Greenstone Belt, NW Russia: implication for basin development and duration of the volcanism, *Precambrian Res.*, 2014, vol. 245, pp. 51–65.

Hart, S.R., Blusztajn, J., Dick, H.J.B., Meyer, P.S., and Muehlenbachs, K., The fingerprint of seawater circulation in a 500-meter section of ocean crust gabbros, *Geochim. Cosmochim. Acta*, 1999, vol. 3, pp. 4059–4080.

Kaulina T.V., Avedisyan A.A., Tomilenko A.A., Ryabukha M.A., and Il'chenko V.L., Fluid inclusions in quartz from uranium mineralization areas of the Litsa ore cluster (Kola Peninsula), *Russ. Geol. Geophys.*, 2017, vol. 58, no. 9, pp. 1059–1069.

Van Keken, P.E., Hauri, E.H., and Ballentine, C.J., Mantle mixing: the generation, preservation, and destruction of chemical heterogeneity, *Annu. Rev. Earth Planet. Sci.*, 2002, vol. 30, pp. 493–525.

Krogh, T.E., A low-contamination method for hydrothermal decomposition of zircon and extraction of U and Pb for isotopic age determination, *Geochim. Cosmochim. Acta*, 1973, vol. 37, pp. 485–494.

Lahtinen, R., Korja, A., and Nironen, M., Paleoproterozoic tectonic evolution, in *Precambrian Geology of Finland—Key to the Evolution of the Fennoscandian Shield*, Lehtinen, M., Nurmi, P.A., and Ramo, O.T., Eds., Amsterdam: Elsevier, 2005, pp. 481–532.

Larionov, A. N., Andreichev, V. A., and Gee, D. G., The Vendian alkaline igneous suite of northern Timan: ion microprobe U–Pb zircon ages of gabbros and syenite, in *The Neoproterozoic Timanide Orogen of Eastern Baltica,* Gee, D. G. and Pease, V., Eds., *Geol. Soc. London Mem.*, 2004, vol. 30, pp. 69–74.

Larionova, Yu.O., Samsonov, A.V., and Shatagin, K.N., Sources of Archean sanukitoids (high-Mg subalkaline granitoids) in the Karelian Craton: Sm–Nd and Rb–Sr isotopic-geochemical evidence, *Petrology*, 2007, vol. 15, no. 6, pp. 530–550.

Ludwig, K.R., PbDat for MS-DOS, version 1.21, *U.S. Geol. Survey Open-File Rept.*, 1991, pp. 88–542.

Ludwig, K.R., SQUID 1.12, A User's Manual. A geochronological toolkit for Microsoft Excel, *Berkeley Geochronol. Center Spec. Publ.*, 2005, pp. 1–22.

Lugwig, K.R., Isoplot/Ex Version 4.1, a geochronological toolkit for Microsoft Excel, *Berkeley Geochronol. Center Spec. Publ.*, 2010, no. 4, pp. 1–76.

Martin, A.P., Condon, D.J., Prave, A.R., Melezhik, V.A., and Fallick, A., Constraining the termination of the Lomagundi–Jatuli positive isotope excursion in the Imandra–Varzuga segment (Kola Peninsula) of the North Transfennoscandian Greenstone Belt by high-precision ID-TIMS, in *Proc. AGU Meet.*, San Francisco, 2010, Abstract #U33A-0010.

McDonough, W.F. and Sun, S.-S., The composition of the Earth, *Chem. Geol.*, 1995, vol. 120, pp. 223–253.

Melezhik, V.A. and Sturt, B.A., General geology and evolutionary history of the early Proterozoic Polmak–Pasvik–Pechenga–Imandra/Varzuga–Ust'Ponoy Greenstone Belt in the northeastern Baltic Shield, *Earth Sci. Rev.*, 1994, vol. 36, pp. 205–241.

Melezhik, V.A., Huhma, H., Condon, D.J., Fallick, A.E., and Whitehouse, M.J., Temporal constraints on the Paleoproterozoic Lomagundi–Jatuli carbon isotopic event, *Geology*, 2007, vol. 35, no. 7, pp. 655–658.

Melezhik, V.A., Prave, A.R., Fallick, A.E., Kump, L.R., Strauss, H., Lepland, A., and Hanski, E.J., *Reading the Archive of Earth's Oxygenation. Volume 1: The Palaeoproterozoic of Fennoscandia as Context for the Fennoscandian Arctic Russia – Drilling Early Earth Project*, Springer, 2013.

Mints, M.V., Glaznev, V.I., Kopalov, A.I., et al., *Rannii dokembrii severo-vostoka Baltiiskogo shchita: paleogeodinamika, stroenie i evolyutsiya kontinental'noi kory* (Early Precambrian of the Northeastern Baltic Shield: Paleogeodynamics, Structure, and Evolution of the Continental Crust), Moscow: Nauchn. Mir, 1996 [in Russian].

Mitrofanov, F.P., Skuf'in, P.K., Bayanova, T.B., Levkovich, N.V., and Smirnov, Yu.P., Rhyodacite porphyry pluton in the early proterozoic Pechenga complex: Evidence from the Kola Superdeep Borehole section, *Dokl. Earth Sci.*, 2001, vol. 380, no. 4 pp. 540 –544.

Negrutsa, V.Z., *Ranneproterozoiskie etapy razvitiya vostochnoi chasti Baltiiskogo shchita* (Early Proterozoic Stages of Development of the Eastern Part of the Baltic Shield), Leningrad: Nedra, 1984 [in Russian].

Nerovich, L.I., Bayanova, T.B., Serov, P.A., and Elizarov, D.V., Magmatic sources of dikes and veins in the Moncha Tundra Massif, Baltic Shield: Isotopic–geochronologic and geochemical evidence, *Geochem. Int.*, 2014, vol. 52, no. 7, pp.548–566.

Predovskii, A.A., Fedotov, Zh.A., and Akhmedov, A.M., *Geokhimiya Pechengskogo kompleksa (metamorfizovannye osadki i vulkanity)* (Geochemistry of the Pechenga Complex (Metamorphosed Sediments and Volcanics)), Leningrad: Nauka, 1974 [in Russian].

Predovskii, A.A., Melezhik, V.A., Bolotov, V.I., et al., *Vulkanizm i sedimentogenez dokembriya severo-vostoka Baltiiskogo shchita* (Precambrian Volcanism and Sedimentogenesis in the Northeastern Baltic Shield), Leningrad: Nauka, 1987 [in Russian].

Samsonov, A.V., Larionova, Yu.O., Salnikova, E.B., Travin, A.V., Stepanova, A.V., Veselovskii, R.V., Arzamastsev, A.A., Egorova, S.V., Erofeeva, K.G., and Stifeeva, M.V., U–Pb, Sm–Nd, Rb–Sr and Ar–Ar isotope systems in minerals from the Paleoproterozoic dolerite sill of the Murmansk Province as a basis for a key paleomagnetic pole ~1.86 Ga, in *Mater. VII Ross. Konf. po izotopnoi geokhronologii "Metody i geologicheskie rezul'taty izucheniya*

izotopnykh geokhronometricheskikh sistem mineralov i porod" (Proc. VII Russ. Isotope Geochronol. Conf. "Methods and Geological Results of the Study of Isotope Geochronological Systems of Minerals and Rocks"), Moscow: Inst. Geol. Rudn. Mest., Petrogr., Mineral., Geokhim. RAN, 2018, pp. 313–316.

Seismogeologicheskaya model' litosfery Severnoi Evropy: Laplandsko-Pechengskii raion (Seismological Model of the Northern European Lithosphere. The Lapland–Pechenga Region), Sharov, N.V., Ed., Apatity: Izd. KNTs RAN, 1997 [in Russian].

Sharkov, E.V. and Smolkin, V.F., The Early Proterozoic Pechenga-Varzuga Belt: a case of Precambrian back-arc spreading, *Precambrian Res.*, 1997, vol. 82, pp. 133–151.

Skuf'in, P.K., Evolution of the volcanism of the ore-bearing Pechenga Zone, Kola Peninsula), *Geol. Rudn. Mestor.*, 1993, vol. 35, pp. 271–283.

Skuf'in, P.K., *Vulkanizm Kol'skogo regiona. Chast' I. Drevnii Pechengsko-Varzugskii zelenokamennyi poyas (vozrast 2500–1700 mln. let)* (Volcanism of the Kola Region. Part I. The Ancient Pechenga–Varzuga Greenstone Belt (2500–1700 Ma)), Lambert Acad. Publ., 2014 [in Russian].

Skuf'in, P.K., *Vulkanizm rannego proterozoya Kol'skogo regiona. Chast' II. Vulkanogennye formatsii pozdnikh karelid Svekofenno-Vepsiiskogo orogennogo poyasa (1905–1700 mln let)* (The Early Proterozoic Volcanism in the Kola Region. Part II. Volcanogenic Formations of Late Karelides of the Svecofennian–Vepsian Orogenic Belt (1905–1700 Ma)), Lambert Acad. Publ., 2018a [in Russian].

Skuf'in, P.K., A new model of geological structure of the Southern zone of Early Proterozoic Pechenga–Varzuga greenstone belt (Kola Peninsula), *Vestn. Kol'sk. Nauchn. Tsentra RAN*, 2018b, vol. 10, pp. 63–80.

Skuf'in, P.K. and Bayanova, T.B., Early Proterozoic central-type volcano in the Pechenga structure and its relation to the ore-bearing gabbro-wehrlite complex of the Kola Peninsula, *Petrology*, 2006, vol. 14, no. 6, pp. 609–627.

Skuf'in, P.K. and Theart, H.F.J., Geochemical and tectono-magmatic evolution of the volcano-sedimentary rocks of Pechenga and other greenstone fragments within the Kola Greenstone Belt, Russia, *Precambrian Res.*, 2005, vol. 141, pp. 1–48.

Skuf'in, P.K., Bayanova, T.B., and Levkovich, N.V., Lamprophyres in the Early Proterozoic volcanic complex of the Pechenga structure, Kola Peninsula, *Petrology*, 1999, vol. 7, no. 3, pp. 289–303.

Skuf'in, P.K., Bayanova, T.B., Mitrofanov, F.P., Apanasevich, E.A., and Levkovich, N.V., The absolute age of granitoids from the Shuoniyavri Pluton in the southern framework of the Pechenga Structure, the Kola Peninsula, *Dokl. Earth Sci.*, 2000, vol. 370, no. 2, pp. 114–117.

Skuf'in, P.K., Bayanova, T.B., and Mitrofanov, F.P., Isotope age of subvolcanic granitoid rocks of the Early Proterozoic Panarechka volcanotectonic structure, Kola Peninsula, *Dokl. Earth Sci.*, 2006, vol. 409, no. 1, pp. 774–778.

Skuf'in, P.K., Elizarov, D.V., and Zhavkov, V.A., Geology and geochemistry of the volcanic rocks of the South Pechenga structural and formational zone, *Vestn. Murmansk. Gos. Tekh. Univ.*, 2009, vol. 12, no. 3, pp. 416–435.

Skuf'in, P.K., Bayanova, T.B., Elizarov, D.V., and Serov, P.A., New isotope–geochemical data on the volcanic sequence of the Pechenga structure, in *Tr. X Vseross. Fersman. Nauch. Sess. "Geologiya i poleznye iskopaemye Kol'skogo regiona," Apatity, 7–10 aprelya 2013 g.* (Proc. X All-Russ. Fersman Sci. Sess. "Geology and mineral resources of the Kola Region), Apatity: Izd. K&M, 2013, pp. 103–107.

Skuf'in, P.K., Bayanova, T.B., and Serov, P.A., Isotopy of rocks of the Por'itash intrusion (Pechenga structure), in *Mater. Mezhd. tekh. konf. "Nauka i obrazovanie-2014,"* (Proc. Int. Tecton. Conf. "Science and Education–2014"), Apatity, 2014, pp. 874–878.

Smolkin, V.F., *Komatiitovyi i pikritovyi magmatizm rannego dokembriya Baltiiskogo shchita* (Komatiite and Picrite Magmatism of the Early Precambrian of the Baltic Shield), St. Petersburg: Nauka, 1992 [in Russian].

Smolkin, V.F., Magmatism of the Early Proterozoic (2.5–1.7 Ga) rift system in the northwestern Baltic Shield, *Petrology*, 1997, vol. 5, no. 4, pp. 350–365.

Smolkin, V.F., The origin and age of gabbro of the Zhdanov deposit of Cu–Ni ores (Pechenga), in *Tez. Konf. "Korrelyatsiya geologicheskikh kompleksov Fennoskandii"* (Proc. Conf. "Correlation of Geological Complexes of the Fennoscandia"), Petrozavodsk: Izd. KarNTs RAN, 1999, pp. 150–151.

Smolkin, V.F., Mitrofanov, F.P., Avedisyan, A.A., Balashov, Yu.A., Balaganskii, V.V., Borisov, A.E., Borisova, V.V., Voloshina, Z.M., Kozlova, N.E., Kravtsov, N.A., Negrutsa, V.Z., Mokrousov, V.A., Petrov, V.P., Radchenko, A.T., Skuf'in, P.K., and Fedotov, Zh.A., *Magmatizm, sedimentogenez i geodinamika Pechengskoi paleoriftogennoi struktury* (Magmatism, Sedimentogenesis, and Geodynamics of the Pechenga Paleorift Structure), Apatity: Izd. Kol'sk. Fil. RAN, 1995 [in Russian].

Smolkin, V.F., Skuf'in, P.K., Mitrofanov, F.P., and Mokrousov, V.A., Stratigraphy and volcanism in the Early Proterozoic Pechenga structure (Kola Peninsula), *Stratigr. Geol. Correl.*, 1996, vol. 4, no. 1, pp. 78–94.

Smolkin, V.F., Lokhov, K.I., Sergeeva, L.Yu., Kapitonov, I.N., Rodionov, N.V., Sergeev, S.A., and Bol'shakov, A.N., New data on geochemistry and isotopy (U–Pb, Lu–Hf, Sm–Nd) Keulik–Kenirim ore-bearing gabbro–peridotite complex, Kola Region, in *Tr. Fersman. Nauch. Sess. GI KNTs RAN* (Proc. Fersman Sci. Sess. Geol. Inst. Kola Sci. Centre Russ. Acad. Sci.), 2014, no. 11, pp. 180–187.

Smolkin, V.F., Hanski, E., Huhma, H., and Fedotov, Zh.A., Sm–Nd and U–Pb isotopic study of the Nyasyukka dike complex, Kola Peninsula, Russia, in *Tr. Karel'sk. Nauchn. Tsentra RAN* (Trans. Karelian Sci. Centre Russ. Acad. Sci.), 2015, no. 7, pp. 74–84.

Smolkin, V.F., Lokhov, K.I., Skublov, S.G., Sergeeva, L.Yu., Lokhov, D.K., and Sergeev, S.A., Paleoproterozoic Keulik–Kenirim ore-bearing gabbro–peridotite complex, Kola Region: A new occurrence of ferropicritic magmatism, *Geol. Ore. Deposits*, 2018, vol. 60, no. 2, pp. 142–171.

Söderlund, U. and Johansson, L., A simple way to extract baddeleyite (ZrO_2), *Geochem. Geophys. Geosyst.*, 2002, vol. 3, no. 2, pp. 1–7.

Stacey, J.S. and Kramers, I.D., Approximation of terrestrial lead isotope evolution by a two-stage model, *Earth Planet. Sci. Lett.*, 1975, vol. 26, no. 2, pp. 207–221.

Steiger, R.H. and Jager, E., Subcomission of Geochronology: convention of the use of decay constants in geo- and cosmochronology, *Earth Planet. Sci. Lett.*, 1976, vol. 36, no. 2, pp. 359–362.

Stepanova, A.V., Salnikova, E.B., Samsonov, A.V., Larionova, Yu.O., Arzamastsev, A.A., and Larionov, A.N., U–Pb geochronology of Early Precambrian mafic rocks of the Kola–Murmansk province of the Eastern Fennoscandia: the dike "bar code" as a basis of paleocontinental reconstruction, in *Mater. VII Ross. Konf. po izotopnoi geokhronologii "Metody i geologicheskie rezul'taty izucheniya izotopnykh geokhronometricheskikh sistem mineralov i porod"* (Proc. VII Russ. Isotope Geochronol. Conf. "Methods and Geological Results of the Study of Isotope Geochronological Systems of Minerals and Rocks), Moscow, 2018, pp. 340–342.

Svetov, S.A., Stepanova, A.V., Chazhengina, S.Yu., Svetova, E.N., Rybnikova, Z.P., Mikhailova, A.I., Paramonov, A.S., Ekhova, M.V., and Kolodei, V.A., Precision (ICP–MS, LA–ICP–MS) analysis of rock and mineral composition of Early Precambrian mafic complexes: An illustration of the method and estimation of results' precision, in *Tr. Karel'sk. Nauchn. Tsentra RAN, Ser. Geol. Dokembriya* (Trans. Karelian Sci. Centre Russ. Acad. Sci., Ser. Precambrian Geol.), 2015, no. 7, pp. 54–73.

Vetrin, V.R., Duration of the formation and sources of the granitoids of the Litsk–Araguba Complex, Kola Peninsula, *Geochem. Int.*, 2014, vol. 52, no. 1, pp. 33–45.

Vetrin, V.R., Turkina, O.M., and Rodionov, N.V., U–Pb age and genesis of granitoids in the southern framing of the Pechenga structure, Baltic Shield, *Dokl. Earth Sci.*, 2008, vol. 419, no. 1, pp. 298–302.

Walker, R.J., Morgan, J.W., Hanski, E.J., and Smolkin, V.F., Re–Os systematics of early Proterozoic ferropicrites, Pechenga Complex, Russia: evidence for ancient ^{187}Os enriched plumes, *Geochim. Cosmochim. Acta*, 1997, vol. 61, pp. 3145–3160.

Wanke, A. and Melezhik, V.A., Palaeoproterozoic sedimentation and stromatolite growth in an advanced intracontinental rift associated with the marine realm: a record of the Neoarchean continent breakup? *Precambrian Res.*, 2005, vol. 140, pp. 1–35.

Williams, I.S., U–Th–Pb geochronology by ion microprobe. Applications of microanalytical techniques to understanding mineralizing processes, *Rev. Econ. Geol.*, 1998, vol. 7, pp. 1–35.

Yakovlev, Yu.N. and Yakovleva, A.K., Mafic dikes and pseudotachylites of the Allarechenskoe area, in *Roi maficheskikh daek kak indikatory endogennogo rezhima* (Mafic Dike Swarms as Indicators of Endogenic Regime), Apatity: Izd. KNTs AN SSSR, 1989, pp. 43–53.

Zagorodnyi, V.G., Predovskii, A.A., and Basalaev, A.A., *Imandra–Varzuga zona karelid: geologiya, geokhimiya, istoriya razvitiya* (Imandra–Varzuga Zone of Karelides: Geology, Geochemistry, and Evolution), Leningrad: Nauka, 1982 [in Russian].

Translated by I. Melekestseva